Magnetic induction studies of interiors

Krishan Khurana[1],

(1) Institute of Geophysics and Planetary Physics and Dept. Earth, Planetary and Space Sciences UCLA, Los Angeles, CA 90095.

The principle behind electromagnetic induction

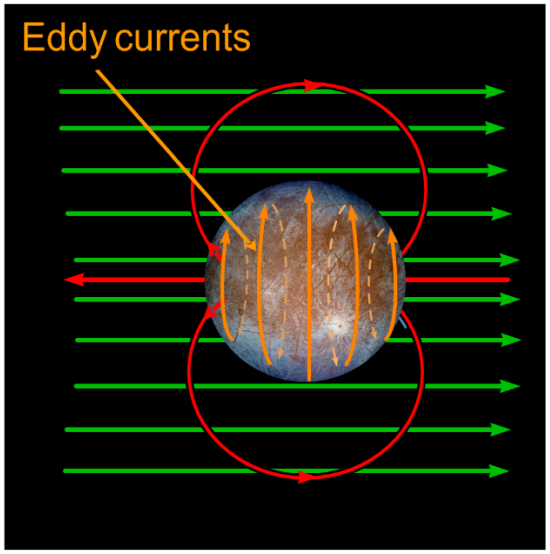

In response to a time-variable **primary field**, **eddy currents** flow on the surface of Europa's ocean creating a dipolar **induced field** that shields Europa's interior from the **primary field**.

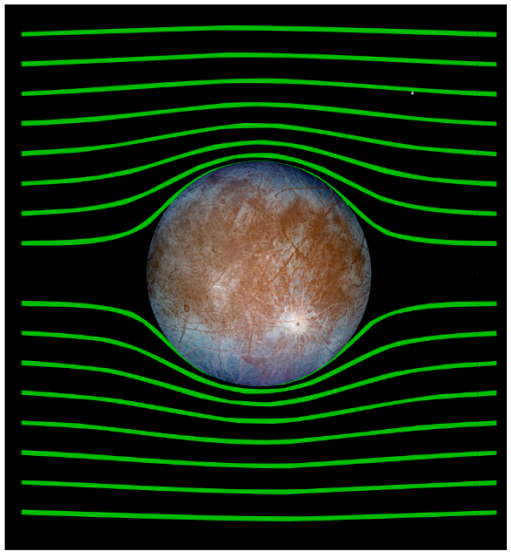

The time-variable primary and induced fields summed together. The varying field circumvents Europa's interior.

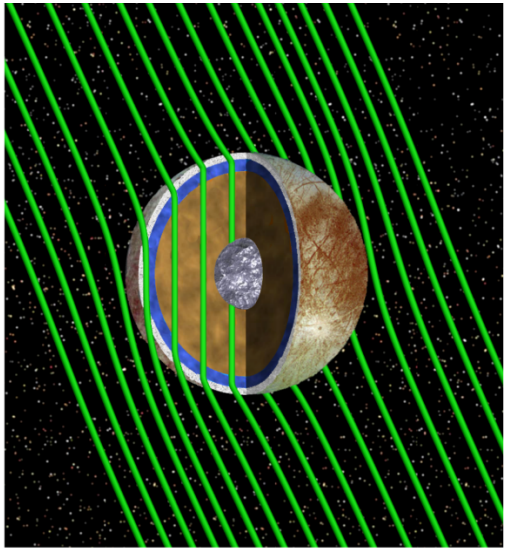

All time-variable and stationary (southward) fields summed together. We model this field.

Amplitude spectrum of the geomagnetic field

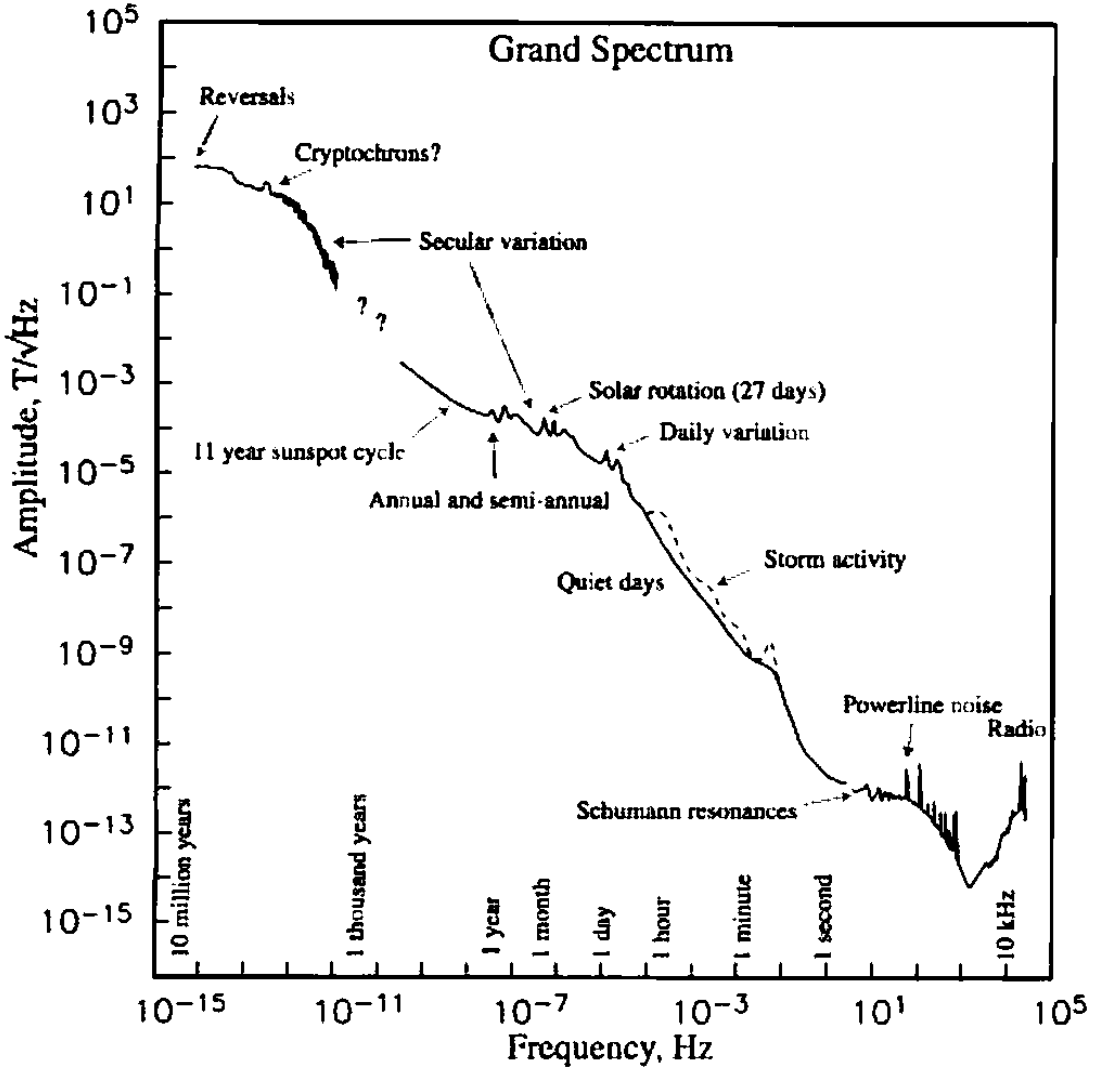

Constable and Constable, 2004

Induction studies of the Earth from satellite data

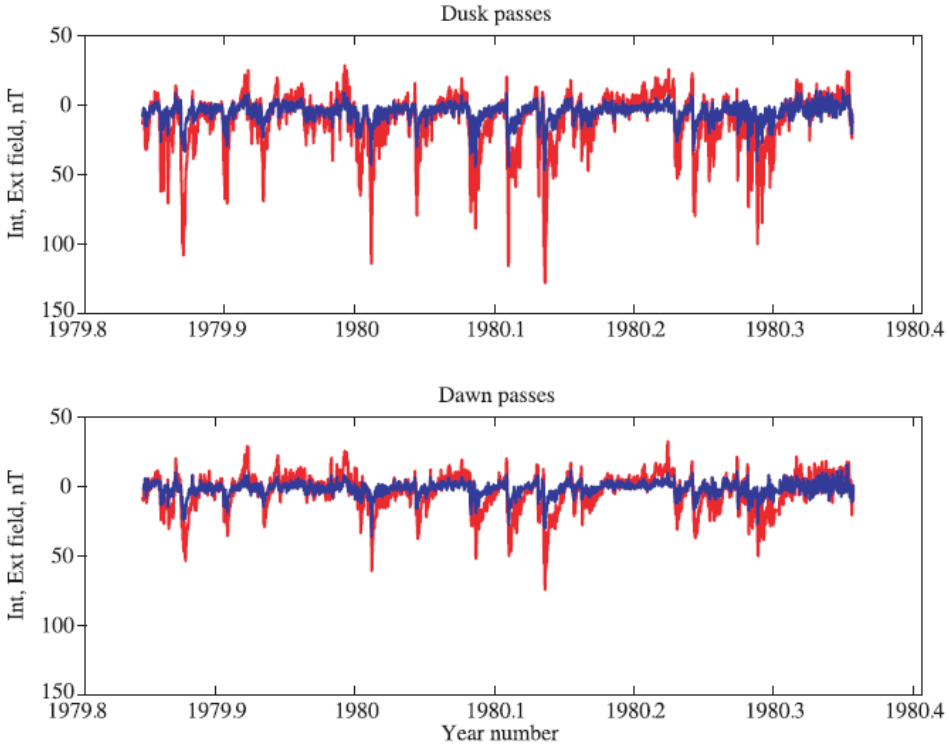

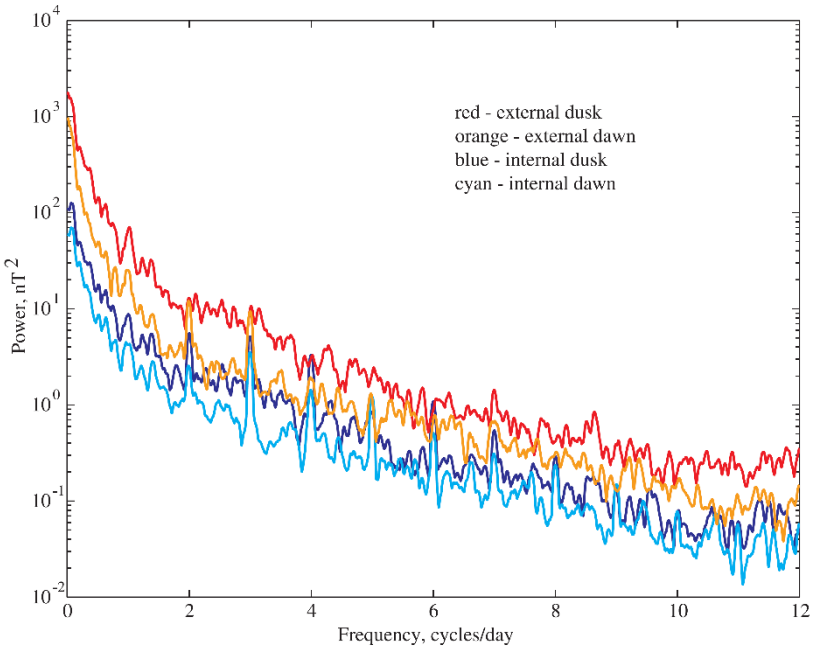

Magsat observations split into external (red) and internal (response) field (blue).

Electromagnetic sounding of the Earth's mantle using surface and space magnetometers

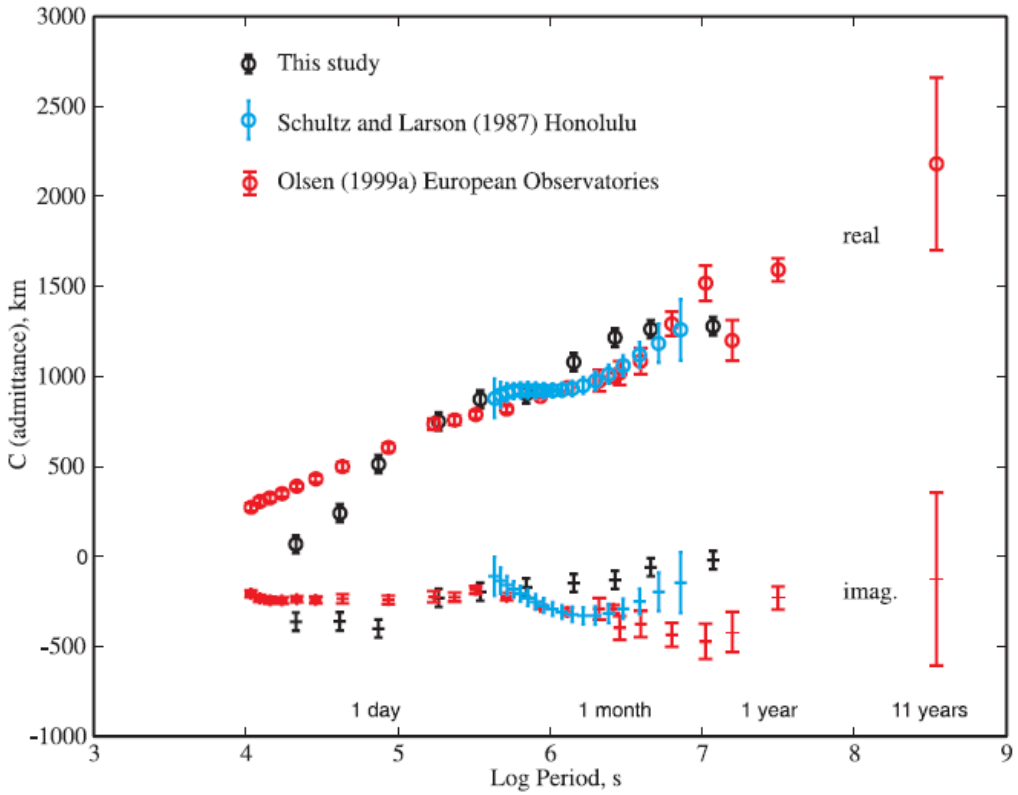

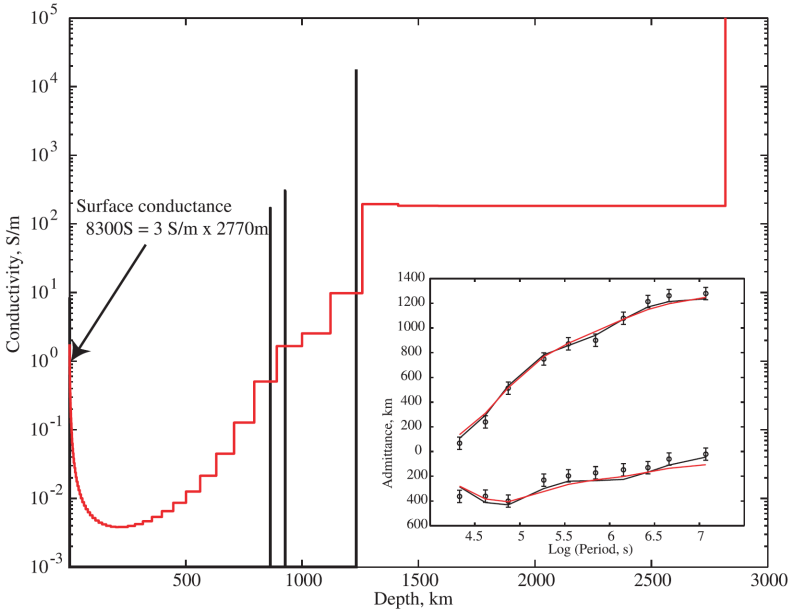

Constable and Constable (2004)

Lunar interior structure from electromagnetic induction

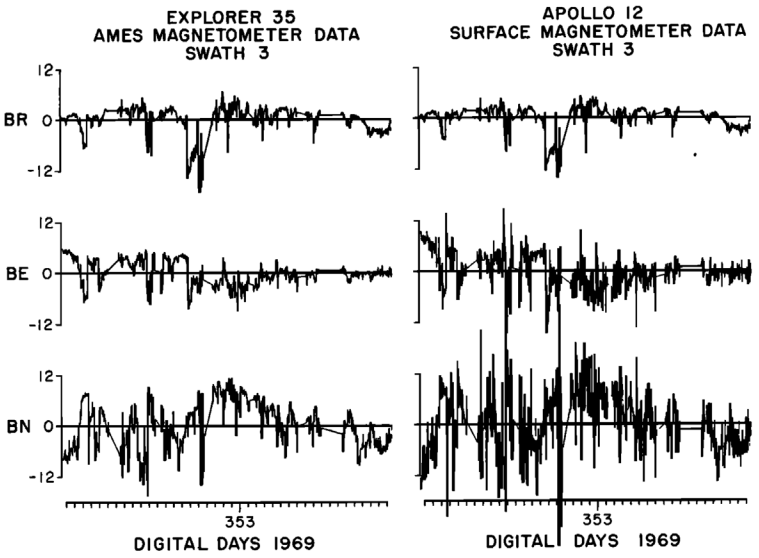

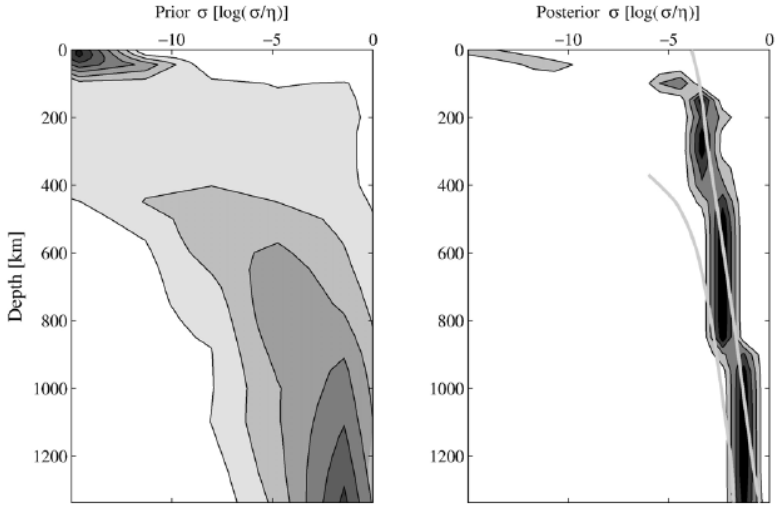

Fig. 7. Marginal prior (left panel) and posterior (right panel) *pdf*'s depicting sampled bulk conductivity profiles as a function of depth from the surface to the CMB. Log signifies base 10 logarithm. Shades of gray as before. Solid gray lines indicate the bounds on conductivity derived by Hood et al. [12].

Khan et al. 2006 (Earth and Planet. Sci. Lett.)

Electromagnetic induction from Mercury's core

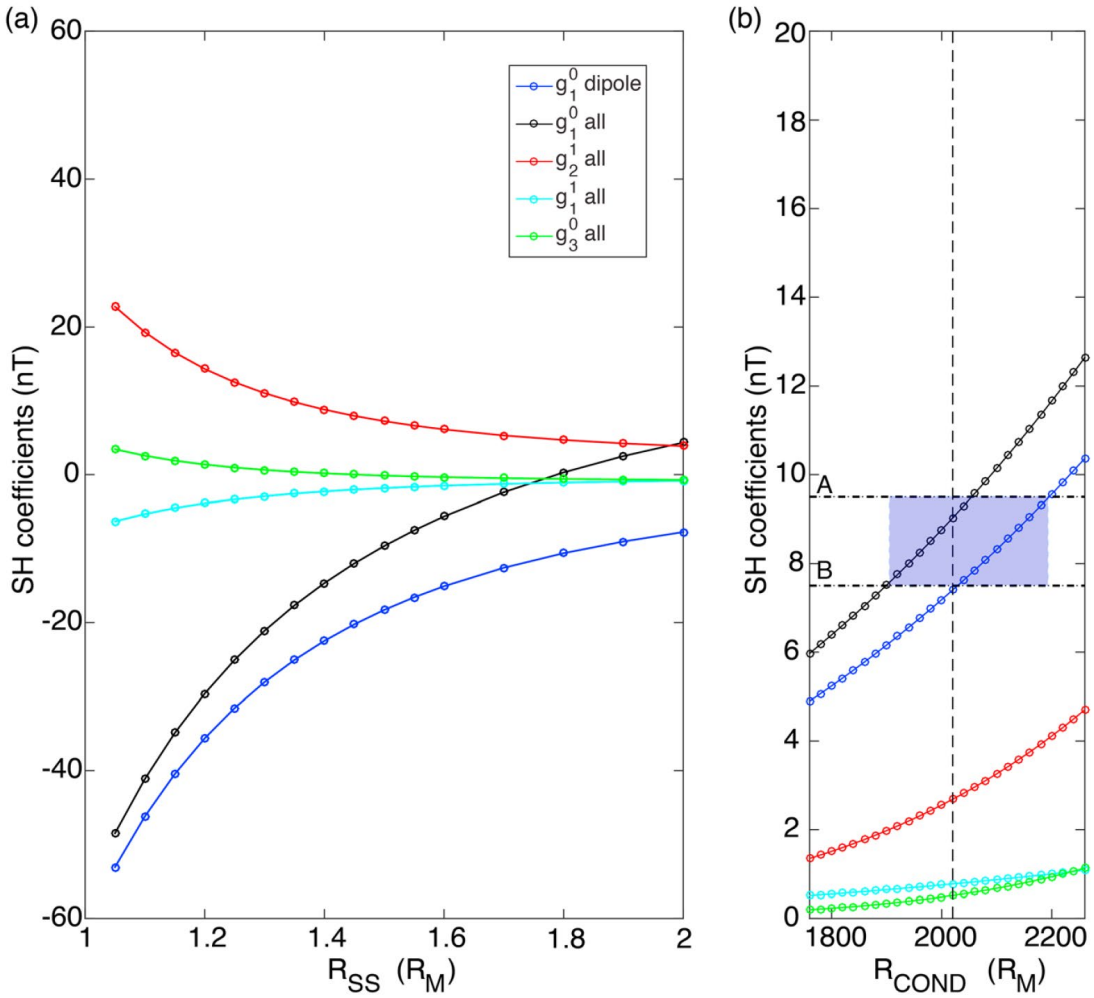

Johnson et al. 2016

For Jovian satellites Jupiter provides the primary field

- The Galilean satellites are located in the inner and middle magnetosphere of Jupiter.
- Because the dipole and rotation axes of Jupiter are not aligned, the moons experience a varying field in their frame.

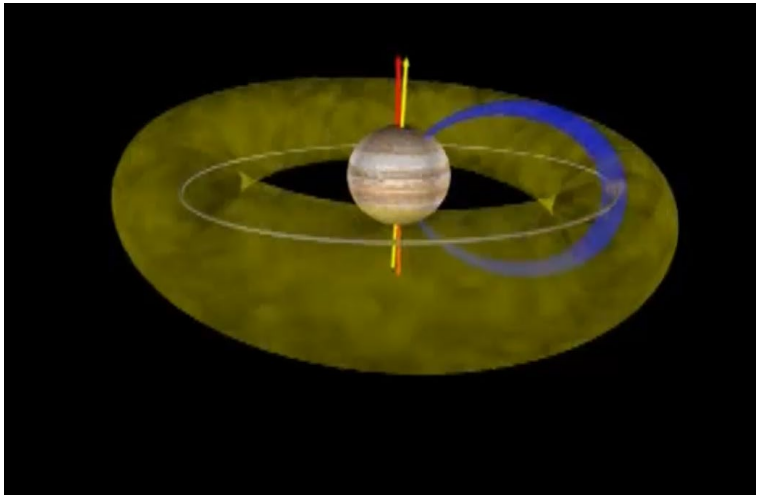

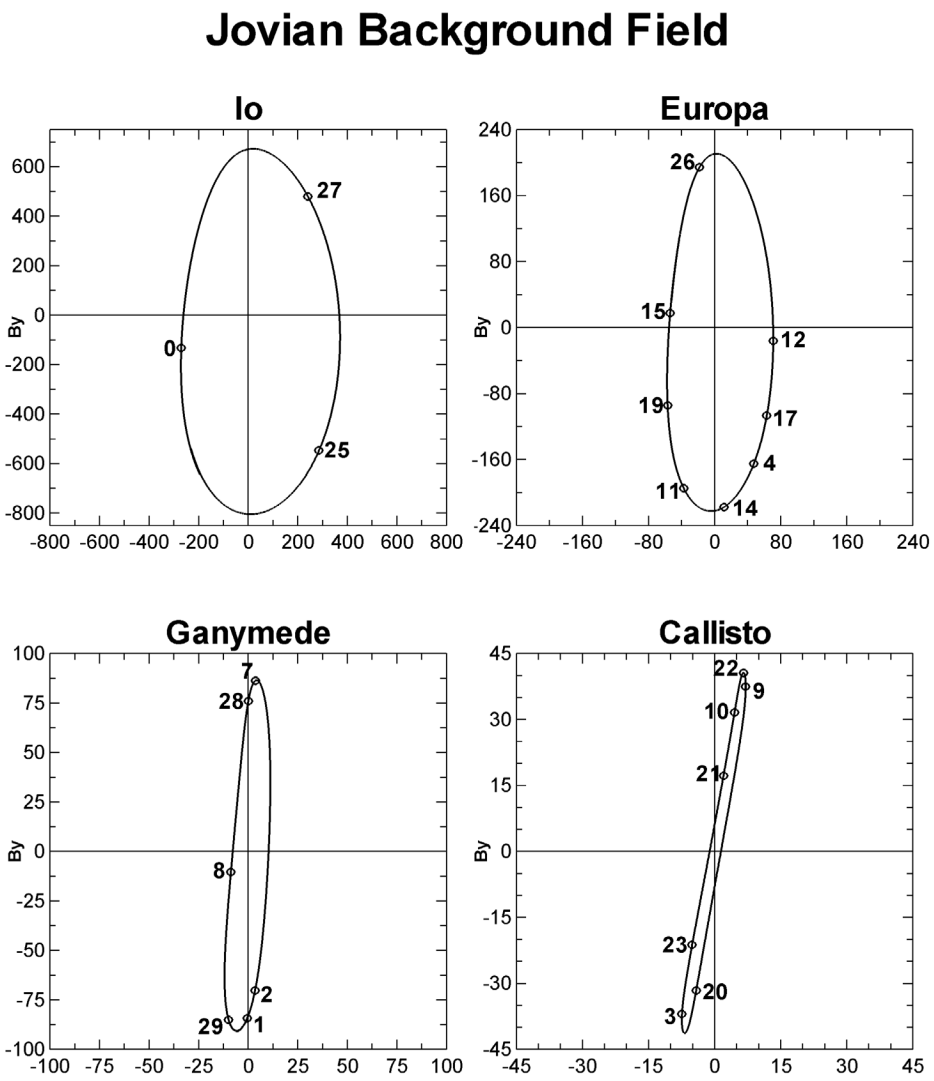

Induction from a finite-conductivity shell

- Because the primary field is uniform and the conductivity distribution has spherical symmetry, the induced field outside the conductor is a dipole field

$$\mathbf{B}_{\text{sec}} = \frac{\mu_0}{4\pi}\left[3(\mathbf{r}\cdot\mathbf{M})\mathbf{r} - r^2\mathbf{M}\right]/r^5 \qquad (1)$$

whose moment **M** oscillates at the same frequency ω and along the same direction $\mathbf{e}_0$ as the primary field. The moment can therefore be written:

so that Eq. 1 becomes:

$$\mathbf{M} = -\frac{4\pi}{\mu_0} A e^{i\phi} \mathbf{B}_{\text{prim}}\, r_{\text{m}}^3/2,$$

- The parameters *A* and *φ* are real numbers, which after Parkinson [1983] are given by the complex equations:

$$\mathbf{B}_{\text{sec}} = -Ae^{-i(\omega t-\phi)} B_{\text{prim}} \left[3(\mathbf{r}\cdot\mathbf{e}_0)\mathbf{r} - r^2\mathbf{e}_0\right] r_{\text{m}}^3/(2r^5)$$

$$Ae^{i\phi} = \left(\frac{r_0}{r_{\text{m}}}\right)^5 \frac{RJ_{5/2}(r_0k) - J_{-5/2}(r_0k)}{RJ_{1/2}(r_0k) - J_{-1/2}(r_0k)}$$

$$R = \frac{r_1 kJ_{-5/2}(r_1k)}{3J_{3/2}(r_1k) - r_1kJ_{1/2}(r_1k)}$$

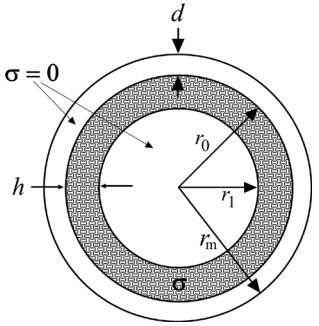

where $k = (1-i)\sqrt{\mu_0\sigma\omega/2}$ has the dimension of a (complex) wave vector, J_m is the Bessel function of first kind and order *m*.

Electromagnetic induction from Europa

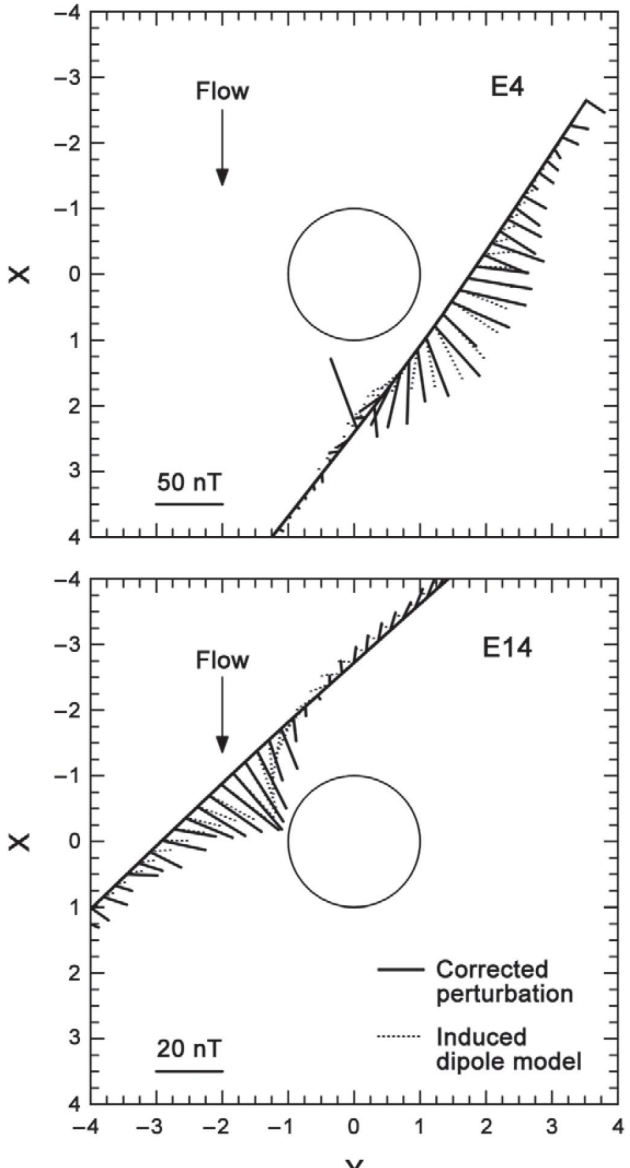

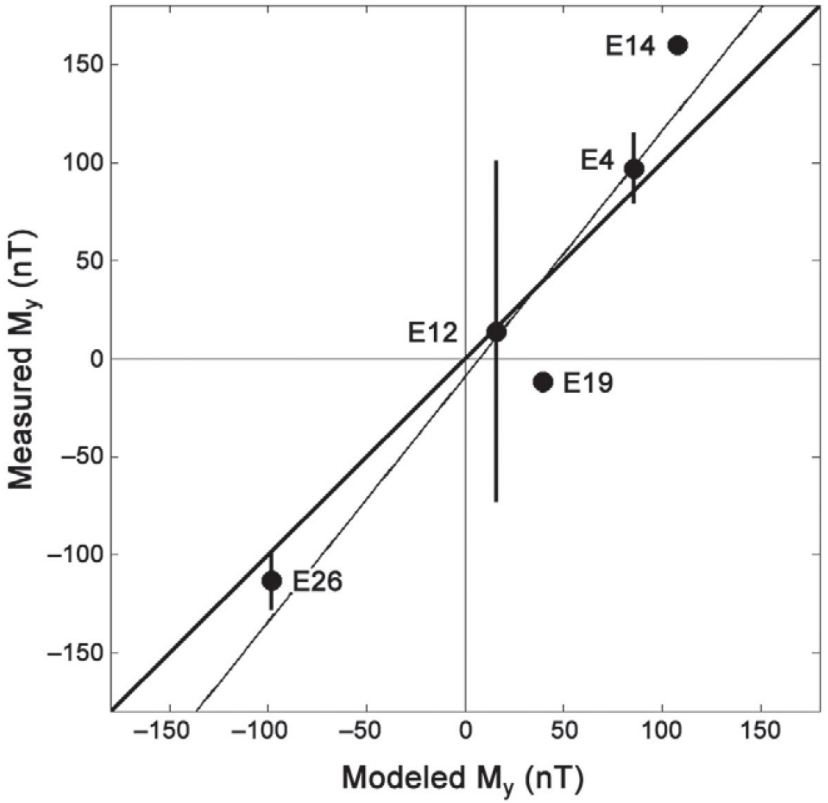

Khurana et al. 1998, Nature

Kivelson et al. 2000, Science

Europa's ice thickness and conductivity

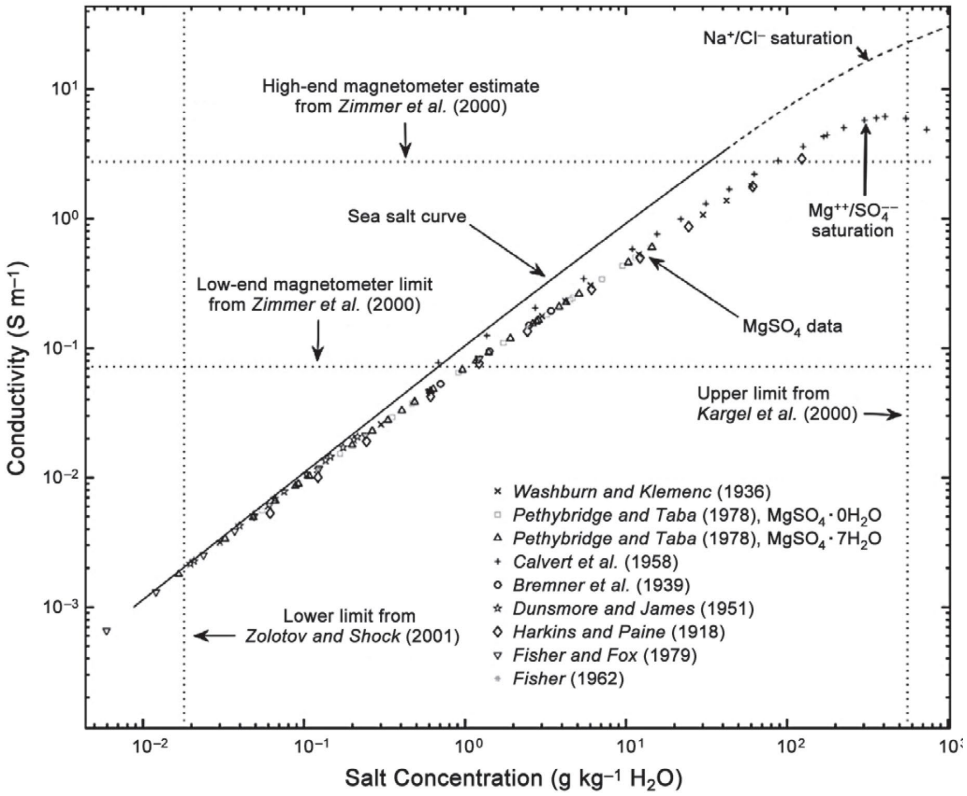

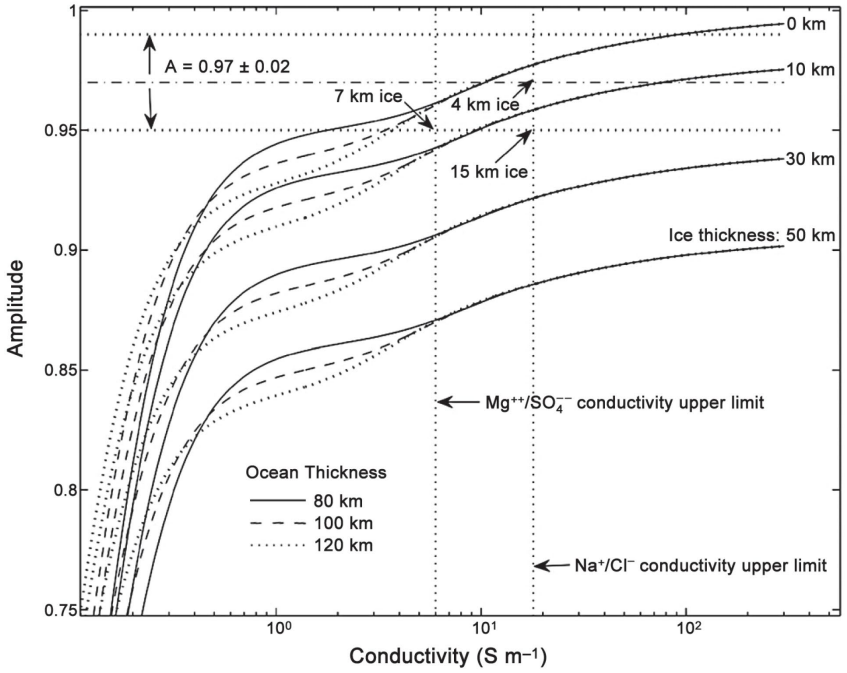

Hand and Chyba, 2007

Jovian Field Spectrum at Europa: Multi-frequency Sounding

- In Europa's rest frame, the external field from Jupiter has many discrete frequencies that can be exploited for multi-frequency induction sounding.

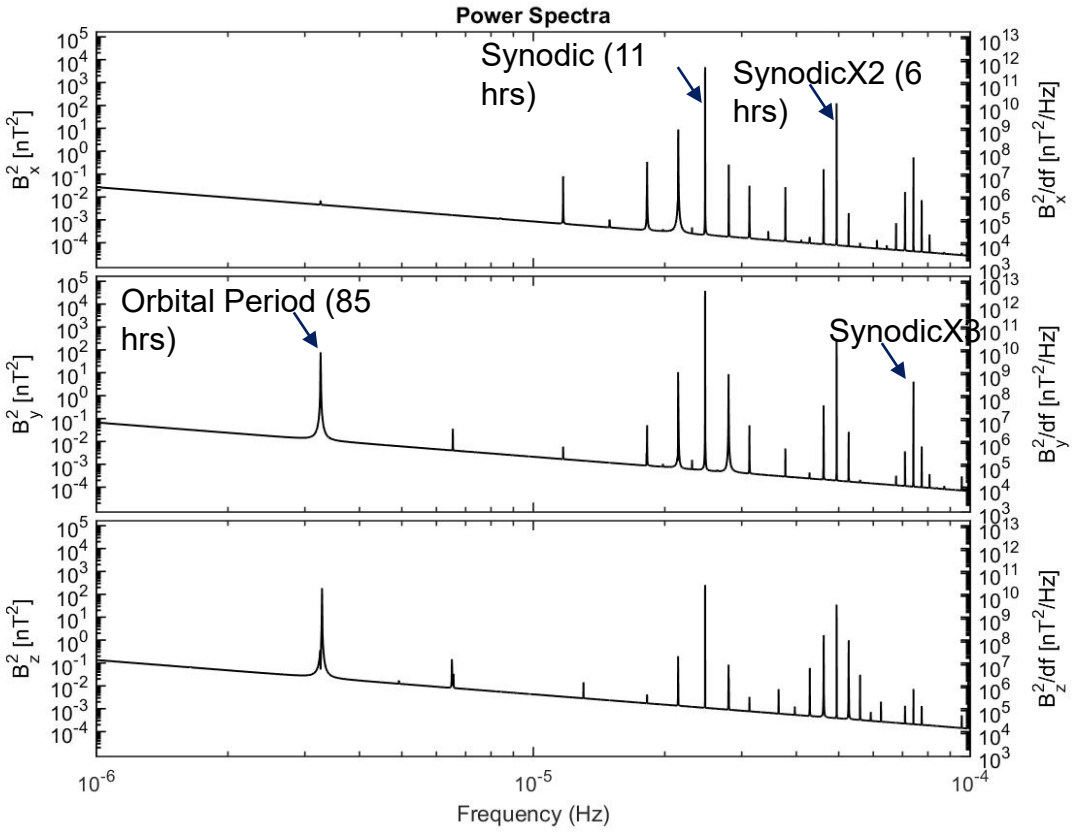

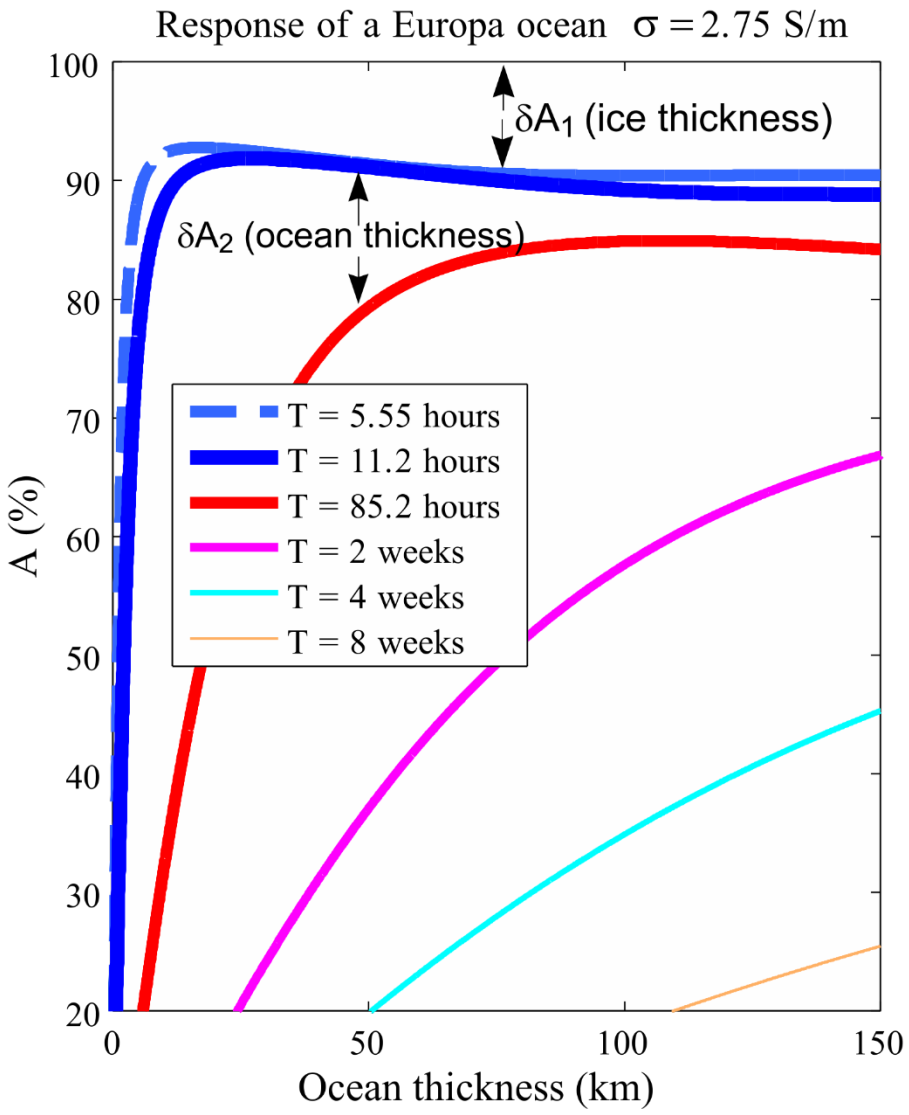

The induction response (efficiency) is stronger for shorter-period waves. Measuring the induction response *A*, at multiple frequencies allows a unique determination of the thickness of the ice shell (using synodic period), and it also constraints the ocean depth (from use of orbital period signal).

Response at synodic period (11.2 hr) provides estimate of ice thickness

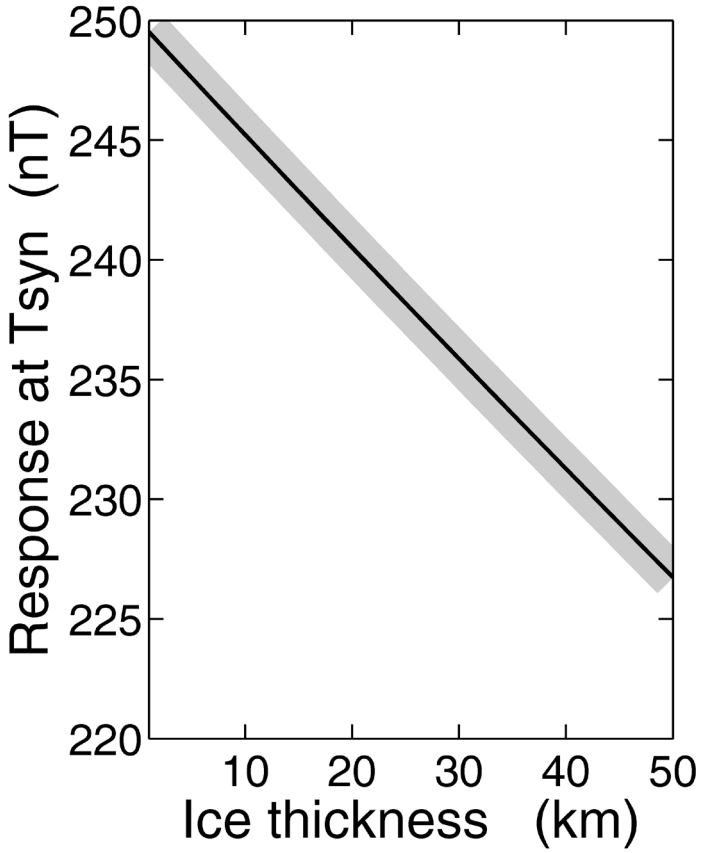

The strength of the secondary field at synodic period falls by 0.5 nT for each km of ice. Thus to determine the ice thickness with a precision of **4 km** would require determining this response with a precision of **2 nT**.

Finding the Ocean Conductivity and thickness

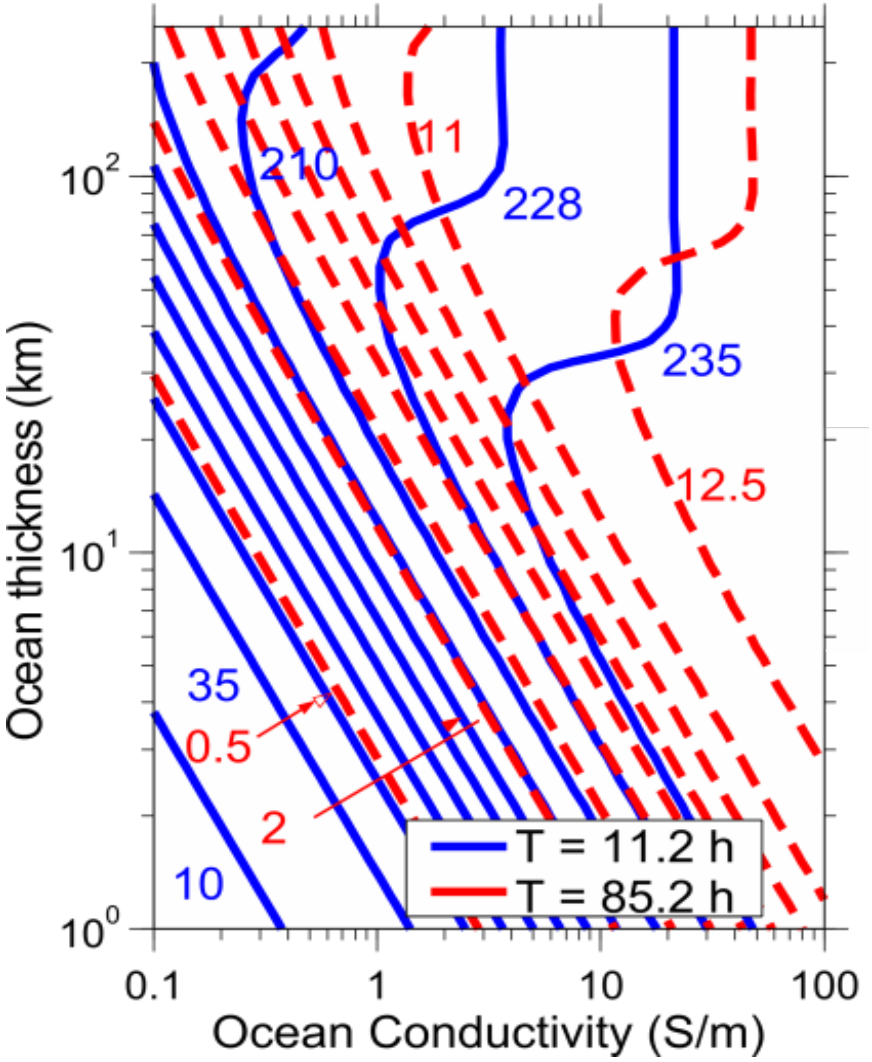

Contours of induced field (in nT) observed at the surface in response to the 11.2–hr (blue, solid lines) and 85.2–hr waves (red, dashed lines) show that responses at these frequencies can uniquely determine ocean parameters in the regime where the contours intersect (large thickness and high conductivity). We would like to determine the orbital period (85.2 hr) response with a precision of **~2 nT.**

Galileo Observations at Callisto

During the C3 flyby, the magnetic field of Jupiter was directed radially outward.

During the C9 flyby, the magnetic field of Jupiter was directed radially inwards.

The observed induction signature also showed opposite polarities.

This confirms that electromagnetic induction and not a permanent dipole is the source of the observed signature.

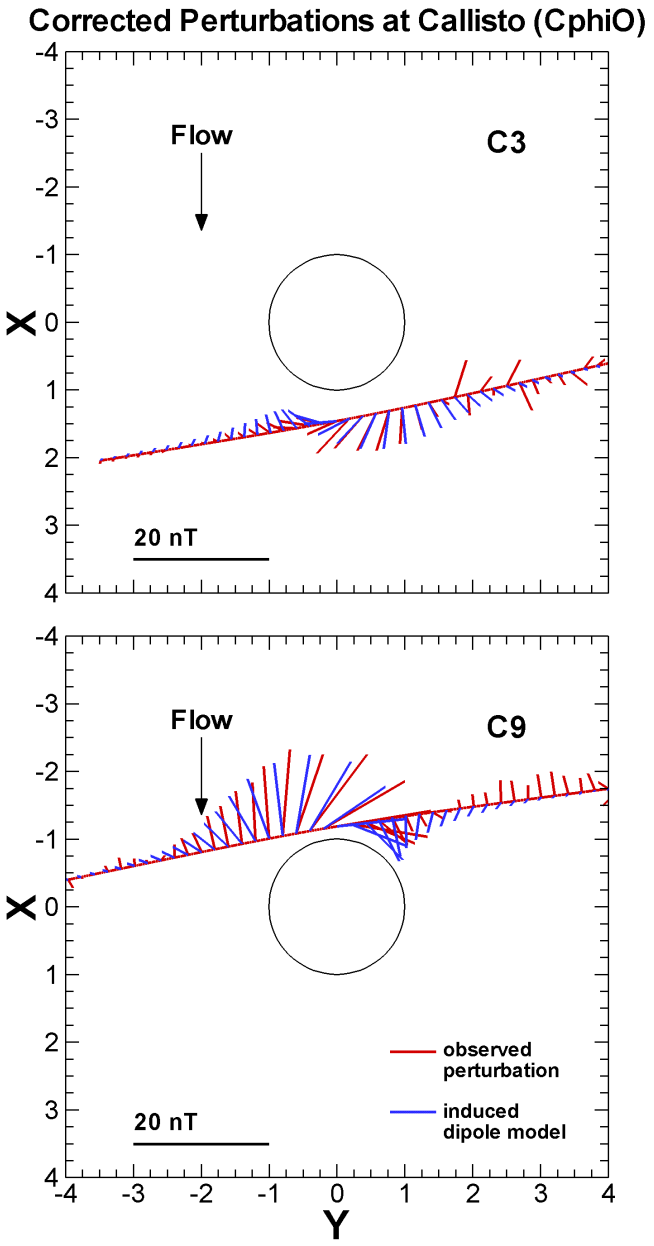

Khurana et al. 1998, Nature

Callisto modelling

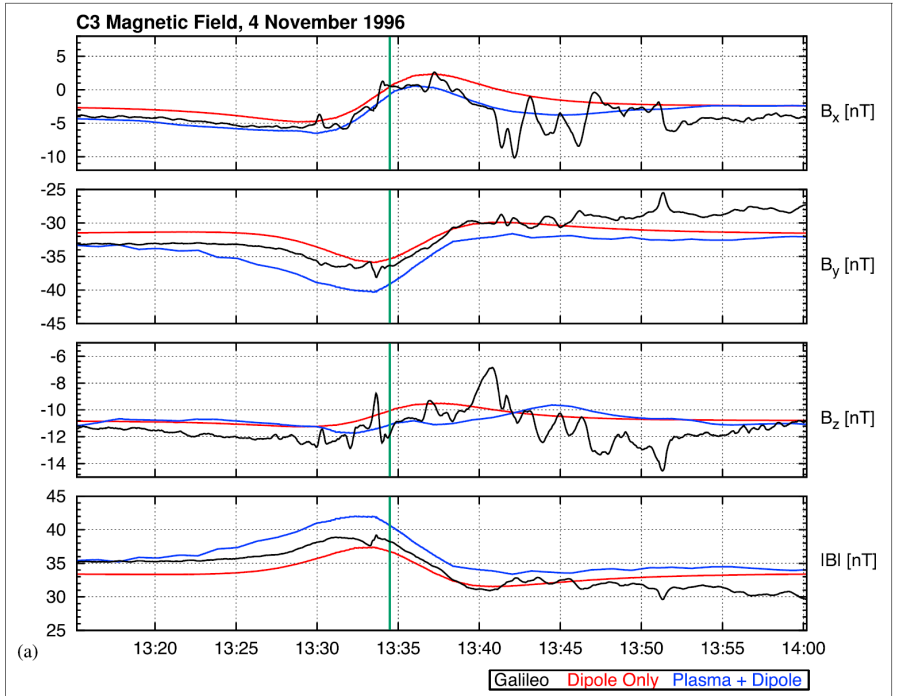

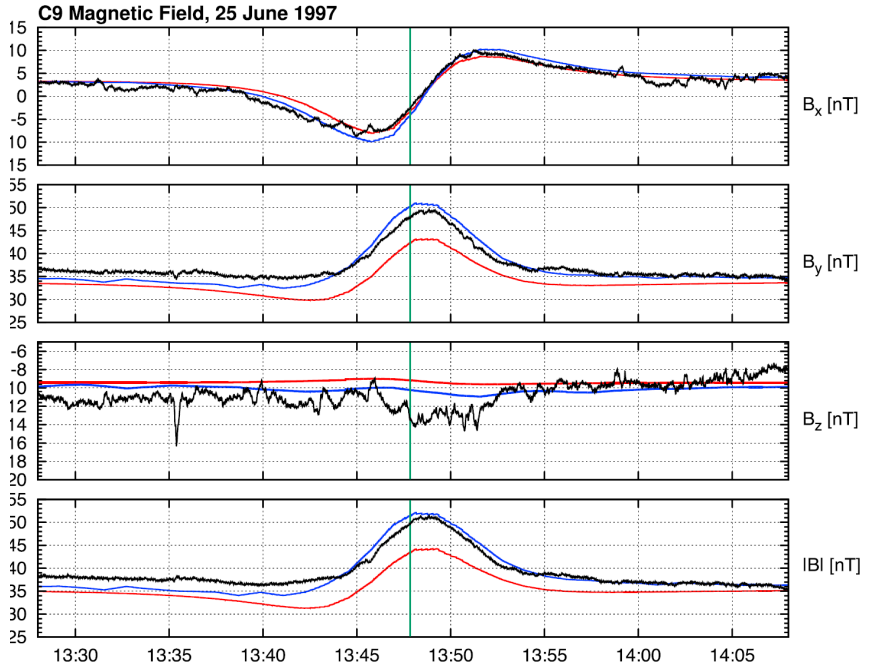

Liuzzo et al. 2015. J.G.R.

Ganymede's magnetosphere

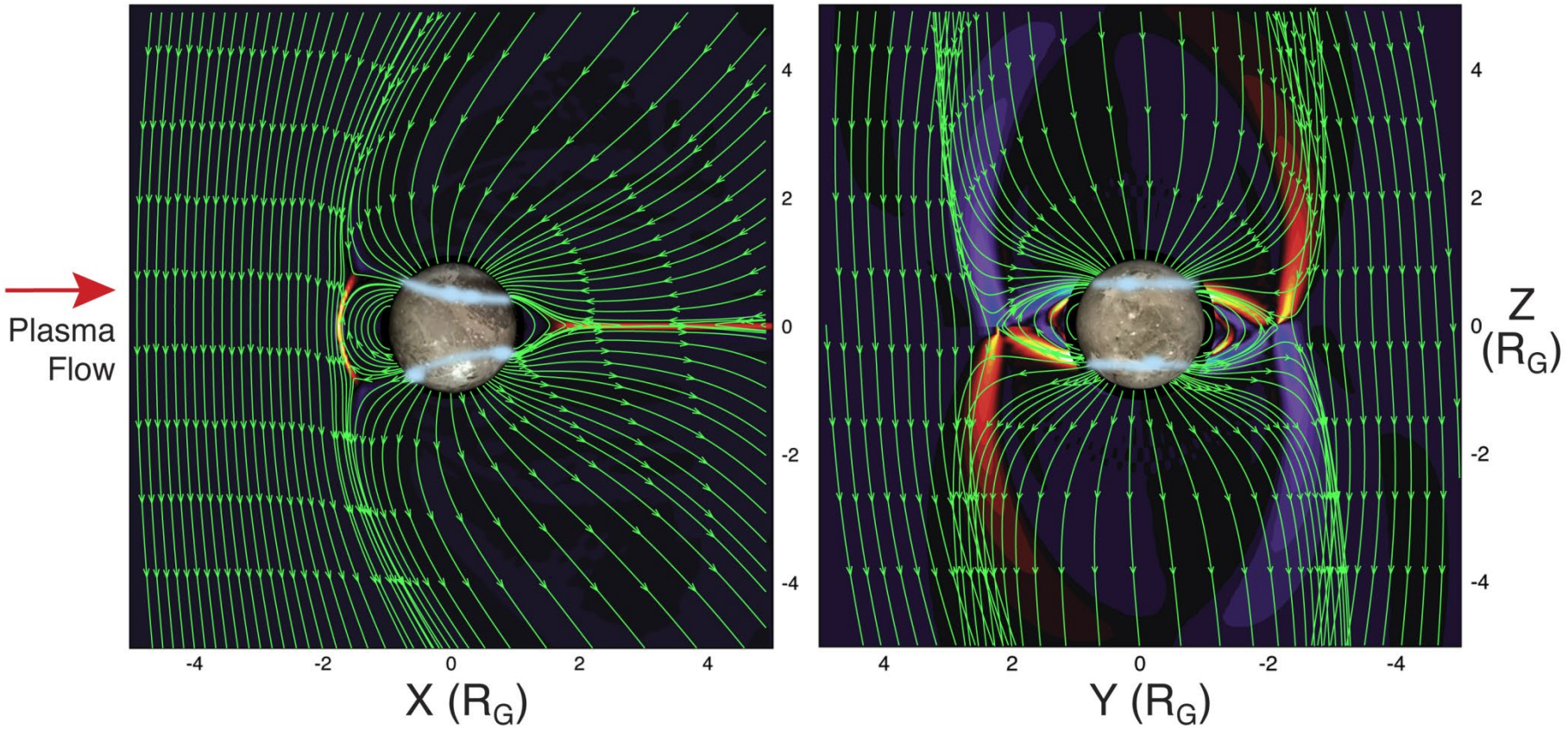

Figure Courtesy: Fran Bagenal, Xianzhe Jia

The inductive response for Ganymede

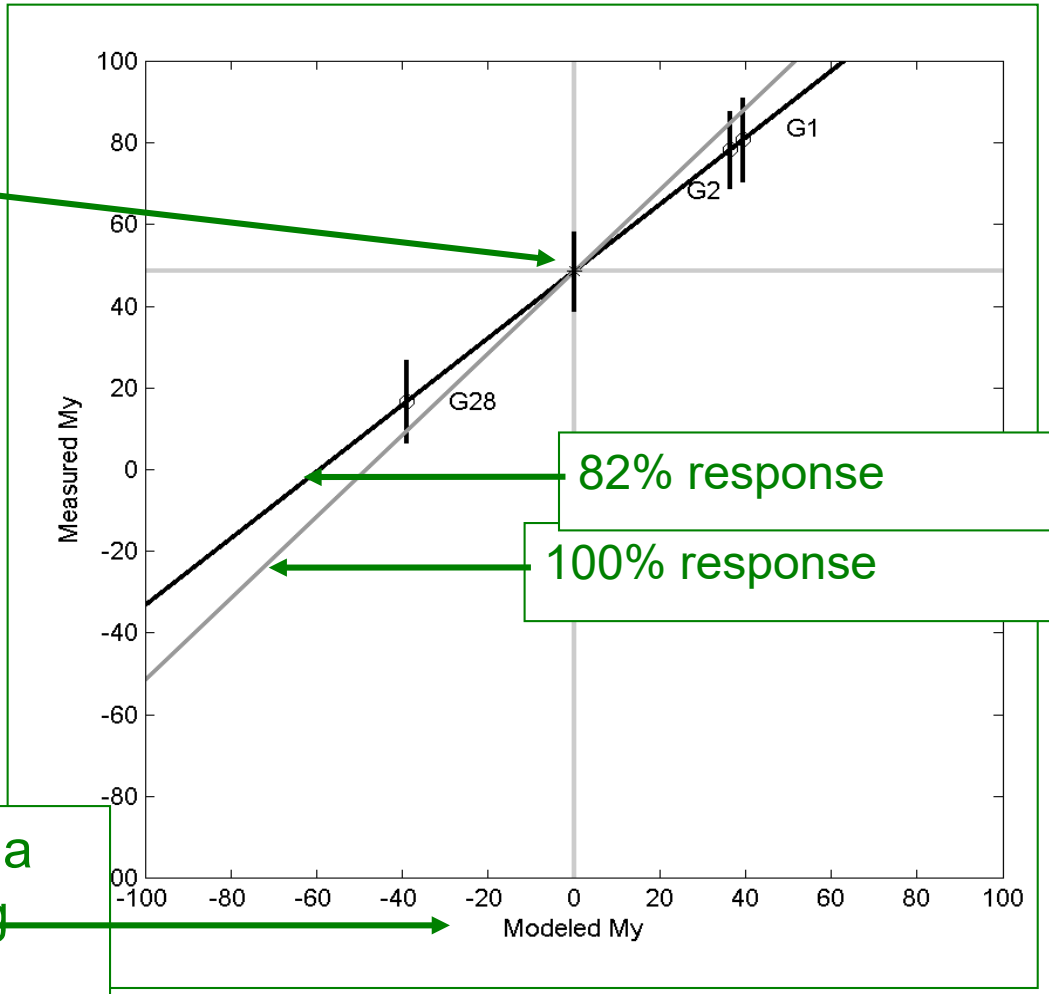

M_{yo} = 49 nT

82% response

100% response

Induced moment in a perfectly conducting sphere

Kivelson et al. Icarus, 2002

Induction from Ganymede is not unambiguous

TABLE VI
RMS Errors and Condition Numbers

See Table	Fitted parameters: Internal dipole	Internal quadrupole	External fields	Inductive response	Summed rms of fit[a]	Summed weighted[b] rms of fit	Condition number	Number of fit parameters
IV	✓		✓		15.1	16.5	12.3	12
V	✓		✓	✓	11.5	13.2	12.5	13
III	✓	✓	✓		13.5	12.6	32.6	17
	✓	✓	✓	✓	13.5	12.6	51.4	18

[a] Units of rms and rmsw are nT.
[b] Data are weighted inversely to the maximum field strength.

Kivelson et al. 2002

Summary of induction from icy Galilean satellites

- "Near" surface conductors are required to fit Europa, Ganymede & Callisto measurements.
- Europa and Callisto induction signatures are global and dipolar suggesting the source is a near surface global conducting shell.
- Source of field cannot be far below the surface because the field strength falls like $(r/R_{surf})^3$ and signature would become too weak to detect.
- We know that Europa's H_2O layer is ~ 150 km thick, Ganymede and Callisto's > 400 km.
- Global sub-surface oceans of at least a few km thicknesses and located at a depth of a few to tens of km for Europa and ~ 150 km for Ganymede and Callisto are required to explain the observed signatures.

Io

How can electromagnetic induction studies help at Io?

Electrical conductivity is a strong function of temperature and melt fraction.

Magnetic field observed near Io can be inverted to obtain the conductivity of Io's interior.

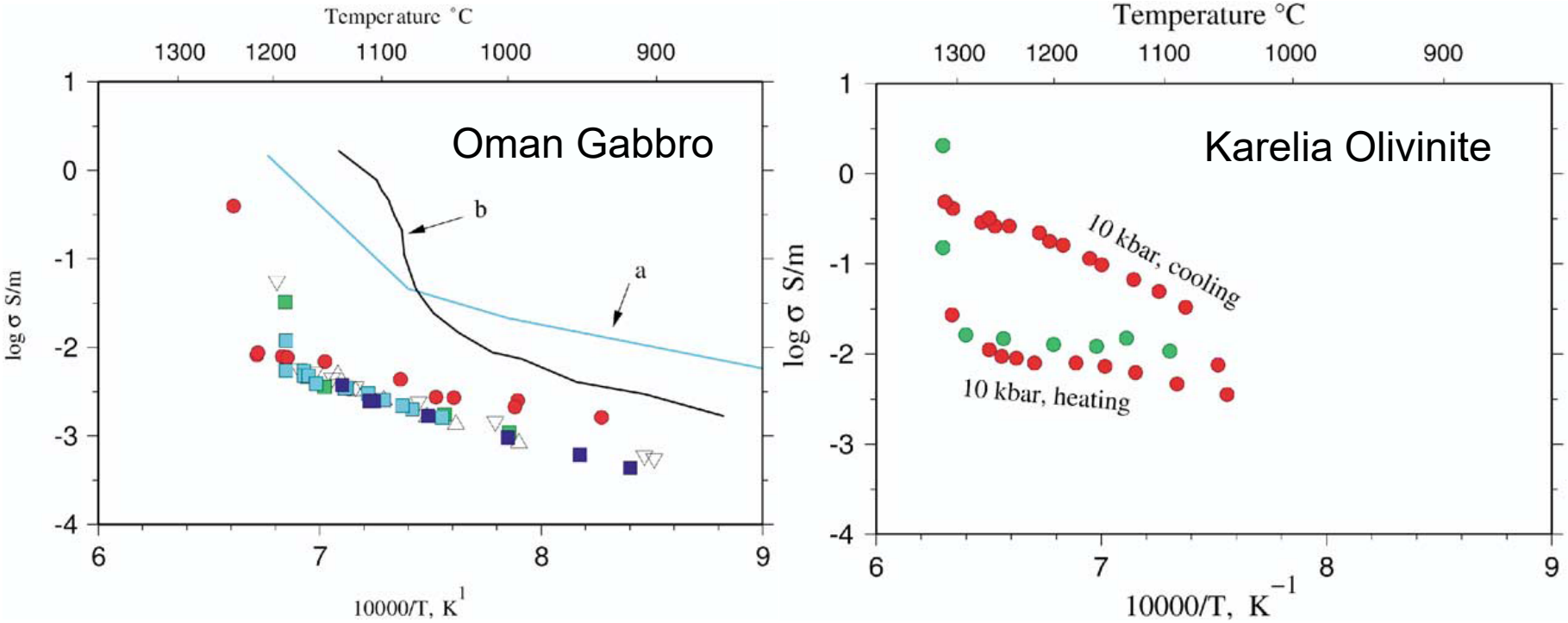

Maumus et al. 2005, Geochimica et Cosmochimica Acta

Rock conductivities: A primer

- The main mechanism of conductivity in solid rocks is temperature-induced semi-conduction involving mobility of mainly conduction band electrons but also ionic mobility aided by point defects.
- For forsterite, electron mobility and more importantly ionic conduction by magnesium vacancies are the main sources of conductivity and near a temperature of 1200 °C its conductivity rises to ~2×10^{-4} S/m.
- For an iron-bearing olivine, an additional source of conductivity arises, namely small polaron hopping (polarization from lattice deformation) of holes from Fe^{3+} to Fe^{2+} on the Mg sublattice which increases the conductivity of the olivine to 10^{-3} S/m at 1200 °C. Thus, the conductivity of an iron-bearing mineral increases with increasing oxygen fugacity (Fe^{3+} abundance).

Rock conductivity increases strongly with temperature: Using magnetometers as thermometers

Conductivity of solid rocks follows an Arrhenius relation (Nover, 2005, Surveys in Geophysics)

$$\sigma = \sigma_0 \exp\left(\frac{-\mathrm{E}_a - P\Delta V}{RT}\right)$$

where, E_a is the activation energy (in Joules) and ΔV is the activation volume (in cm^3 /mol) .

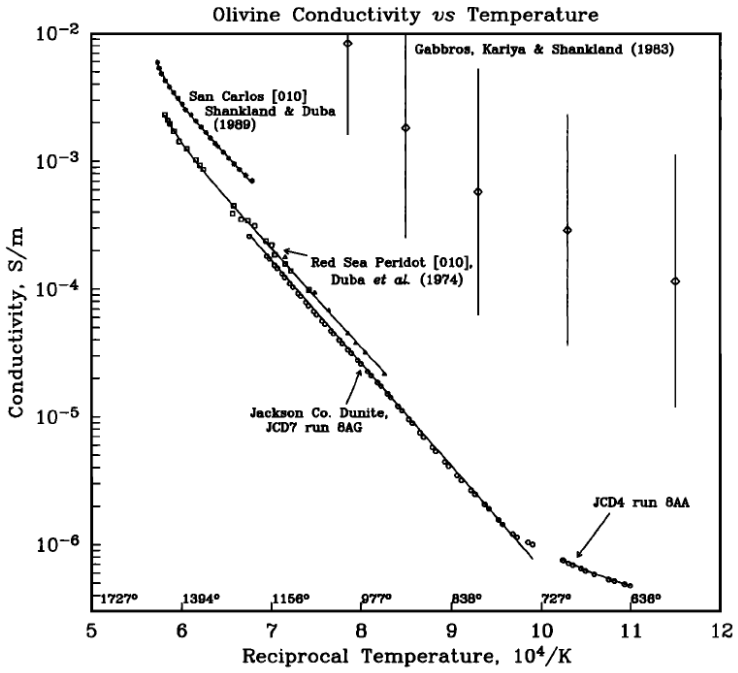

Constable and Duba 1990, JGR

Molten rocks have very “high” conductivity

Table 9. Melt conductivity needed to model the measured molten rock conductivity with Hashin-Strikman upper bound (Eqn. 8).

Sample	$T_{quenching}$ (°C)	log (σ_{solid}) (S/m)	σ_{melt} (S/m)	X_{melt} (vol.%)	log (σ_{HS^+}) (S/m)	log (σ_{mes}) (S/m)
Oman gabbro						
1 GPa	1240	–2.08	1.5	34	–0.41	–0.4
0.5 GPa	1188	–2.24	0.29	15	–1.44	–1.45
0.5 GPa	1187	–2.25	0.31	12	–1.51	–1.5
0.3 GPa	1196	–2.22	0.48	17	–1.20	–1.2
Karelia olivinite, 1 GPa	1315	–1.92	28.8	10	0.30	0.3
Spitzbergen lherzolite						
2 GPa	1465	–1.86	4.9	22	–0.10	–0.1
1 GPa	1360	–2.25	2.5	14	–0.60	–0.6
Ronda lherzolite, 1 GPa	1377	–2.25	2.0	11	–0.80	–0.8
Ol + basalt sample, 1 GPa	1183	–3.06	2.9	4.5	–1.05	–1.05

Maumus et al. 2005

Conductivity of a partial melt depends on many factors

- Conductivities of solid and melt phases of the rocks.
- Dihedral wetting angle, the contact angle between the melt and the adjoining crystal grains . Even for very small melt portions, interconnected melt is observed at grain edges and grain boundaries in thin sections of quenched samples if dihedral angle < 60°.

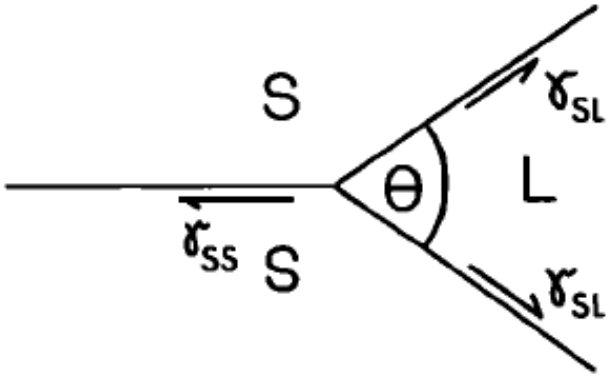

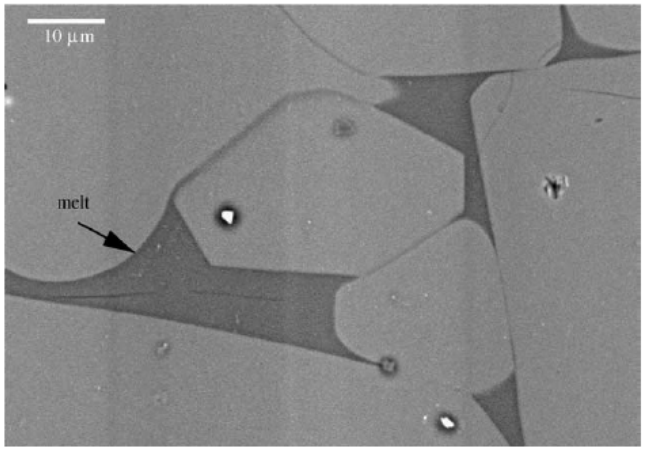

Scanning electron micrograph of Spitzbergen, lherzolite

- The interconnectivity of the melts on a macro scale.

Conductivity of a partial melt: interconnectivity on macro scale

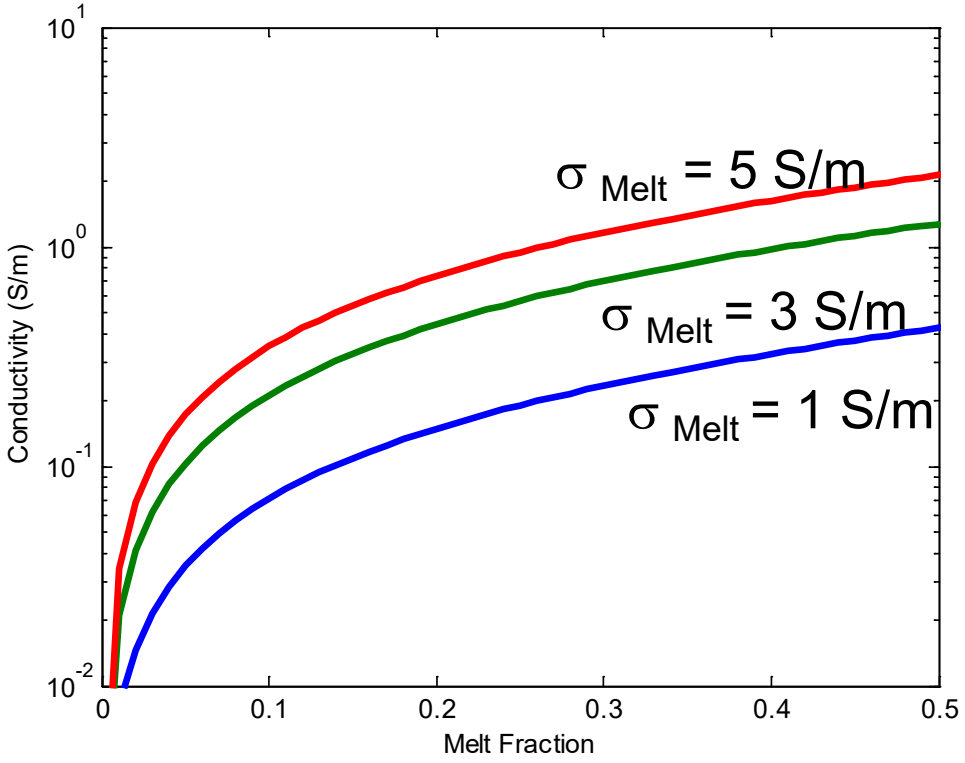

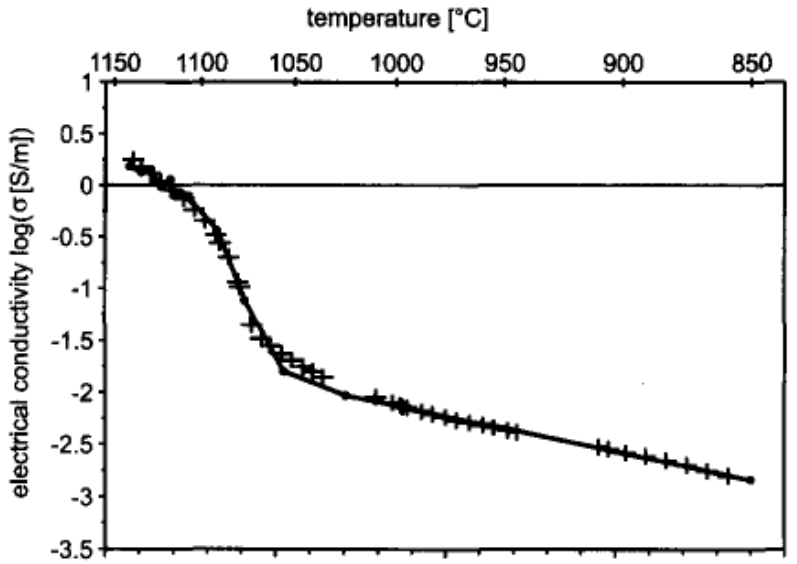

Conductivity of a magnetite partial melt

$$\sigma = \frac{\sigma_l\left(\sigma_l\left(f^{2/3}-1\right)-\sigma_s f^{2/3}\right)}{\sigma_s\left(f-f^{2/3}\right)+\sigma_l\left(f^{2/3}-f-1\right)}$$

Schilling et al. 1997, Physics of Earth and Planet. Interiors

Where x is volume melt fraction, f = 1-x, σ_1 is conductivity of the melt and σ_s is the conductivity of the solid rock

Composition of Io's interior

- Io's bulk composition is believed to be broadly chondritic (L or LL) and as Io has fully differentiated, most of the iron has segregated into its core making its mantle ultramafic but low in Fe.
- After removing a 30-50 km crust rich in silicates and an Fe core of 1000 km radius, the three main constituents of the mantle are SiO_2, MgO and FeO with weight% of 44.1, 32.2 and 14.1 (Keszthelyi et al. 2007).
- A good Earth-analogue for this type of rock is a lherzolite derived from Spitzbergen, Norway.
- Lherzolites are ultramafic igneous rocks rich in olivine and pyroxenes and are believed to be derived from the Earth's upper mantle (Blatt, H. and Tracy R. J., 1996).

Lherzolite from Eifel, France

Jupiter provides the primary field

- Io is located in the inner magnetosphere of Jupiter.
- Because the dipole and rotation axes of Jupiter are not aligned, Io experience a varying field in its frame at a period of 12.953 hrs.
- We will focus on I24, I27 I31 and I32 flybys for which inducing fields were large and changed in polarity.

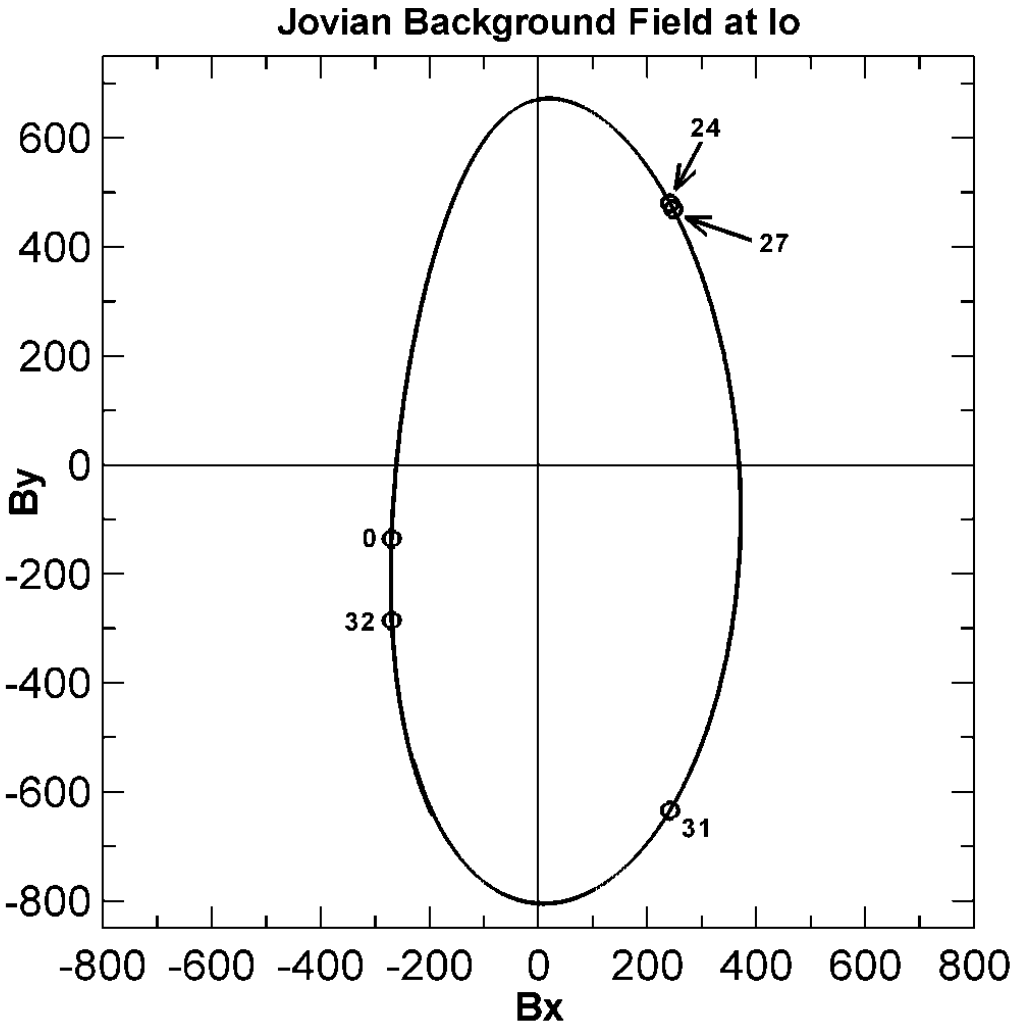

Three layer model

- Assume crust thickness d = 50 km electrically insulating
- r_m = 1820 km
- r_0 = 1770 km
- Core radius r_1 = 600 – 900 km with 0 and ∞ conductivity.
- Mantle thickness h = r_0 - r_1 = 870 – 1170 km with a range of conductivities.

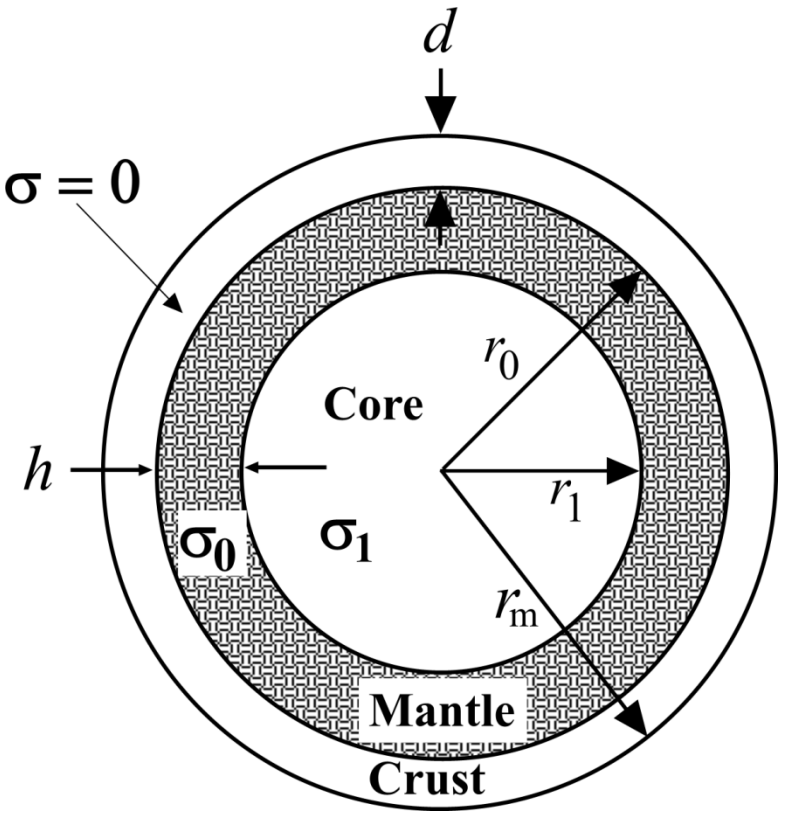

T_{syn}= 12.953 hrs, B_{syn} = 850 nT

T_{orb}= 42.46 hrs B_{orb} ~ 50 nT

Induction from core alone

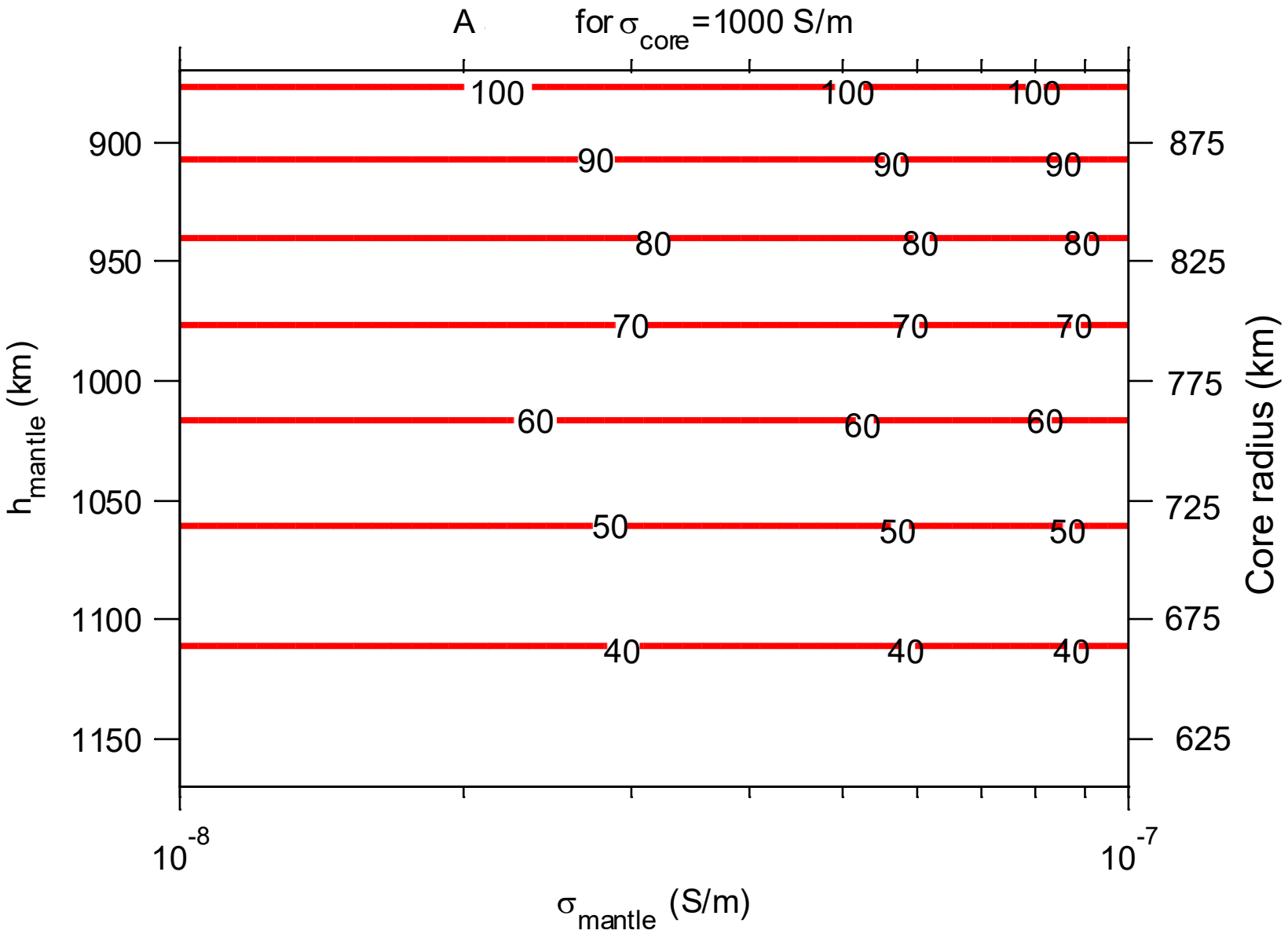

Induction from core + mantle
Extended range plot

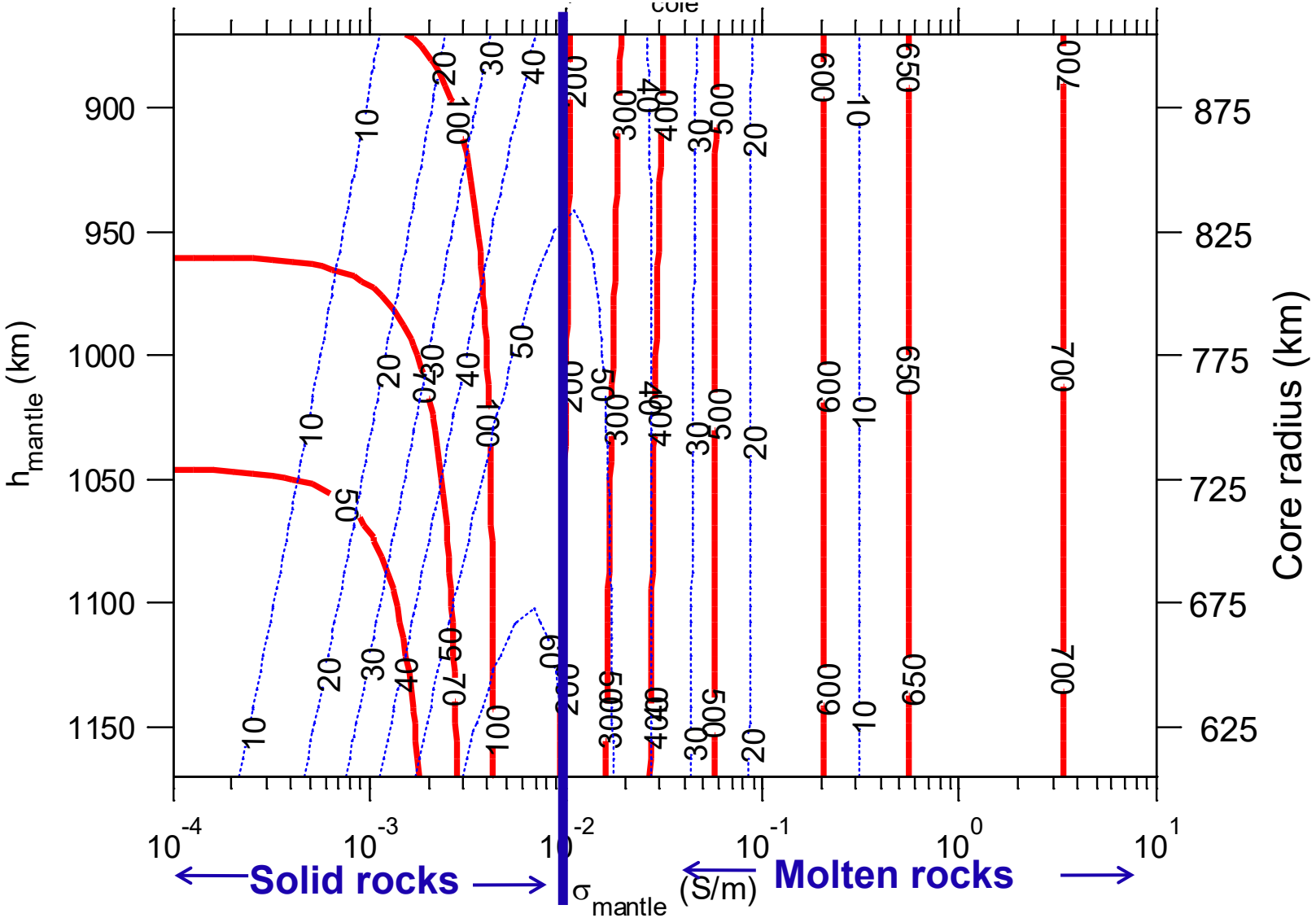

Sources of magnetic field near Io

- Jupiter + its current sheet
  - Obtained from Khurana (1997) magnetospheric model.

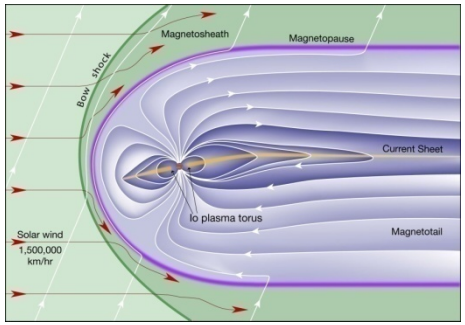

- Plasma interaction currents
  - Calculated from 3-D MHD simulations

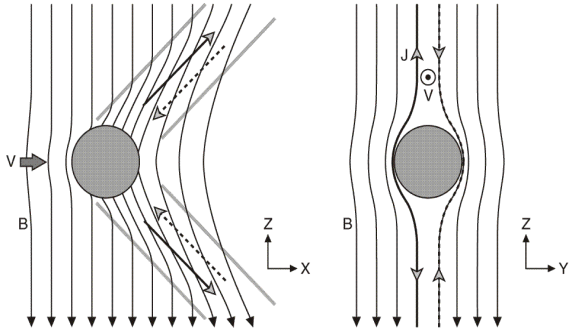

- Electromagnetic induction from a subsurface conductor.
  - Obtained from 3 layer spherical shell models.

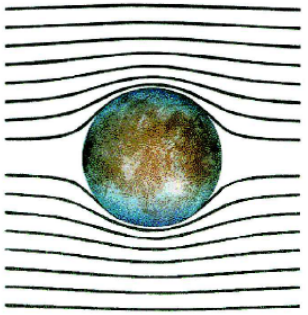

- Permanent internal field
  - Obtained from modeling of residual field

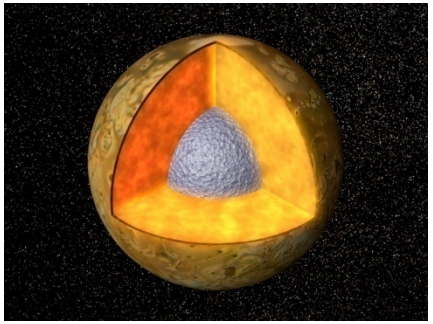

Data MHD model

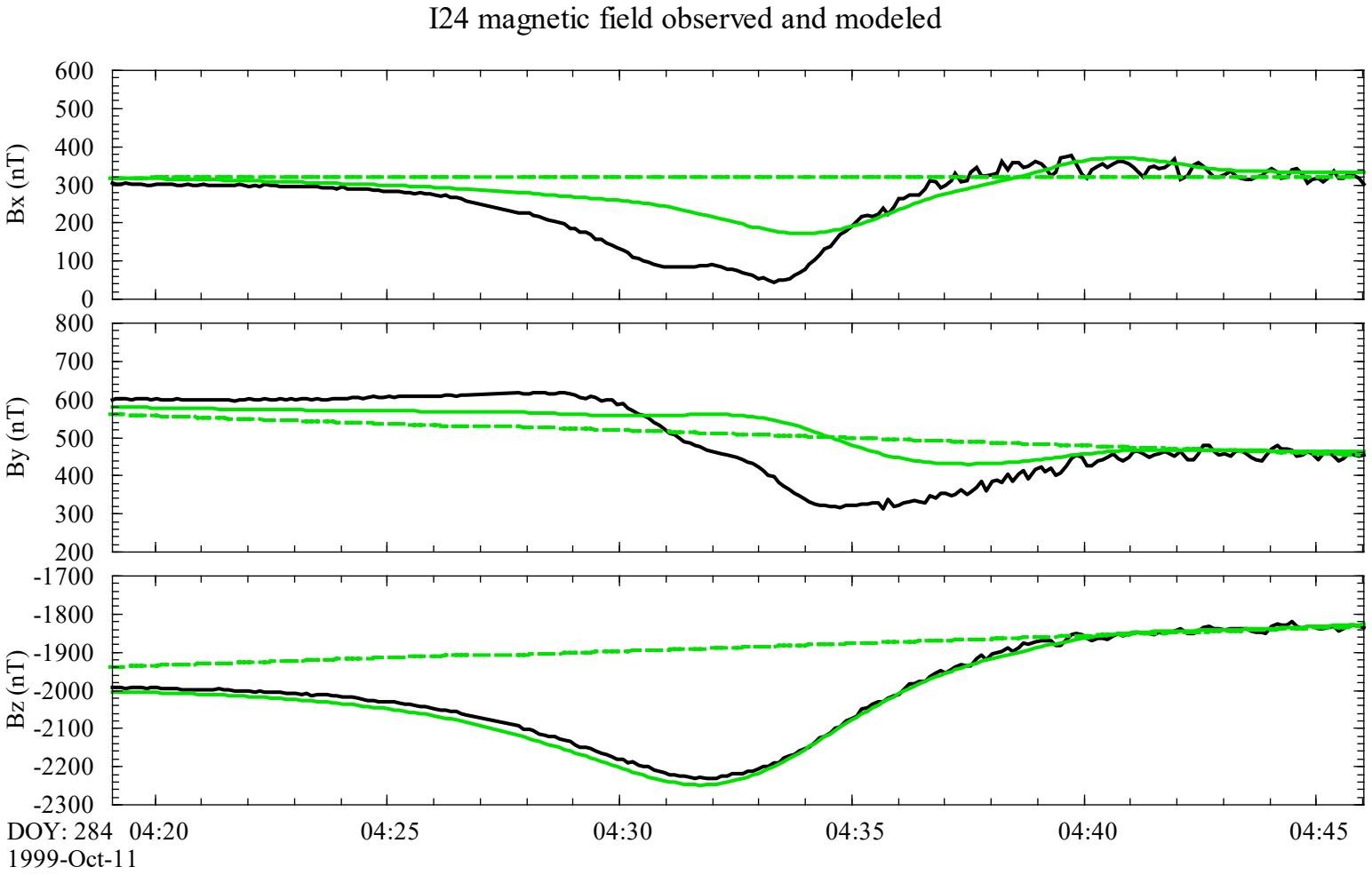

Induction from solid mantle

- We will first consider two models of solid mantle:
  - Warm solid mantle composed of lherzolite (T = 1200 °C) has conductivity = 0.002 S/m.
  - Hot solid mantle (T = 1400 °C) has conductivity = 0.007 S/m.
- Used spherical shell solutions of the electromagnetic diffusion equation in terms of Bessel functions to compute the induction response (Parkinson, 1983).

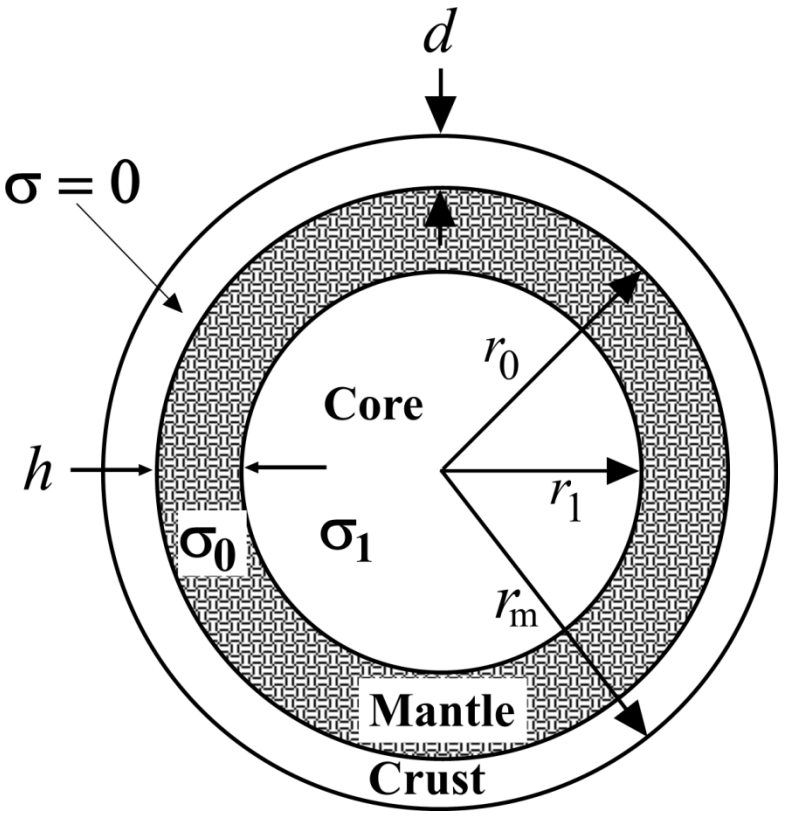

T_{syn}= 12.953 hrs, B_{syn} = 850 nT

T_{orb}= 42.46 hrs B_{orb} ~ 50 nT

I24 Data, MHD, solid mantle models

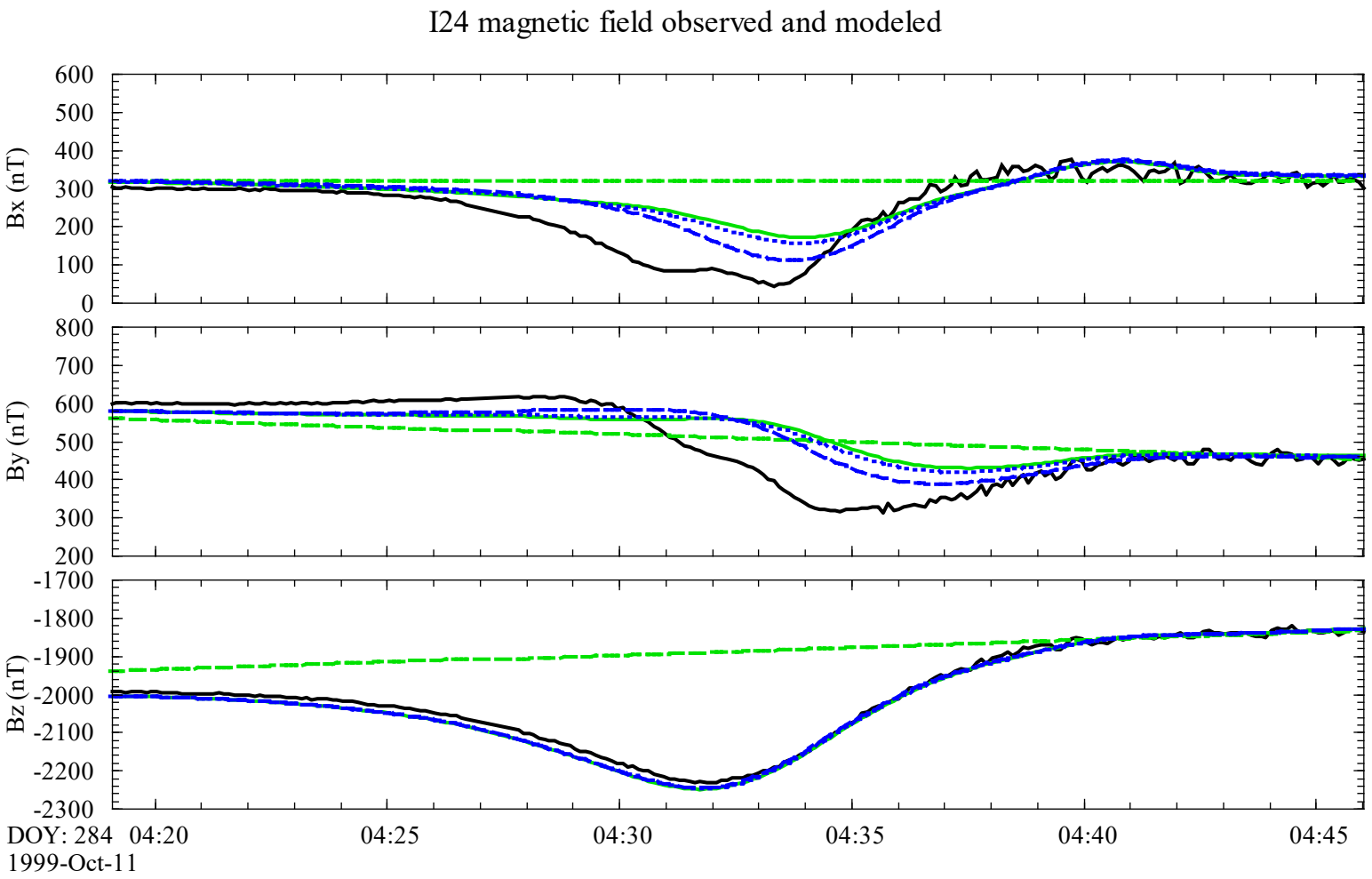

Curves for solid mantle are for warm (1200 °C, dotted lines) and hot (1400 °C, dashed lines) mantle models. The electromagnetic induction from a solid mantle is inadequate to explain the observed signal.

We shall next consider models of a magma ocean (asthenosphere) overlying the solid mantle (and core)

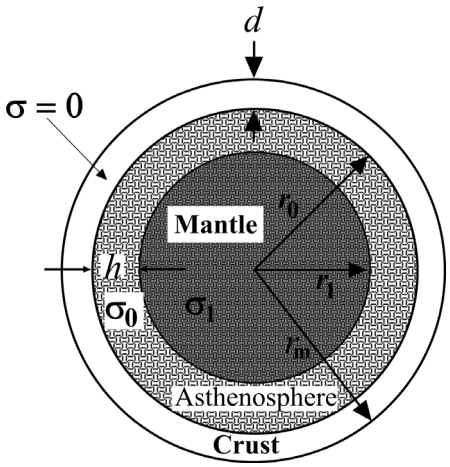

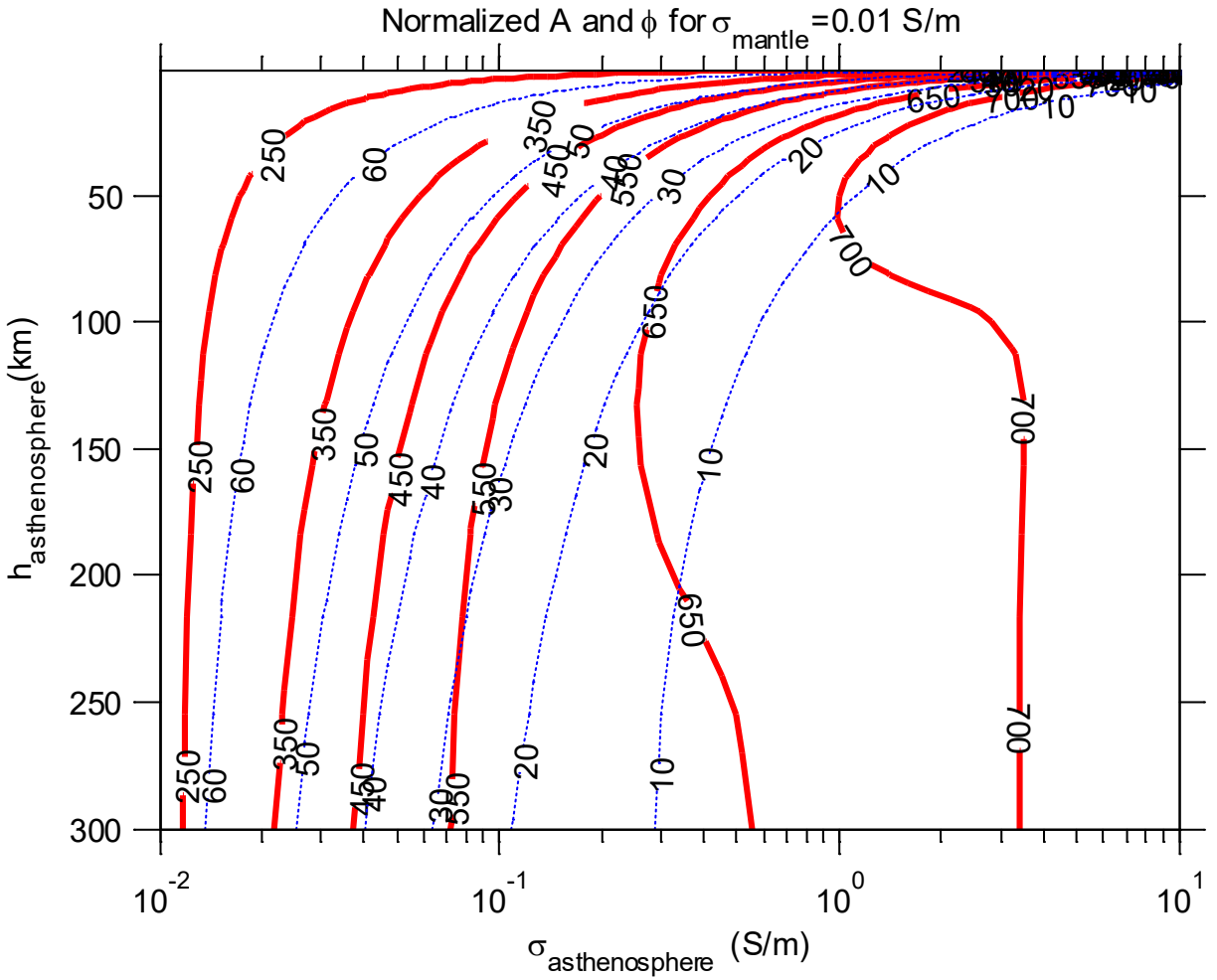

Conductivity of a partial melt of lherzolite

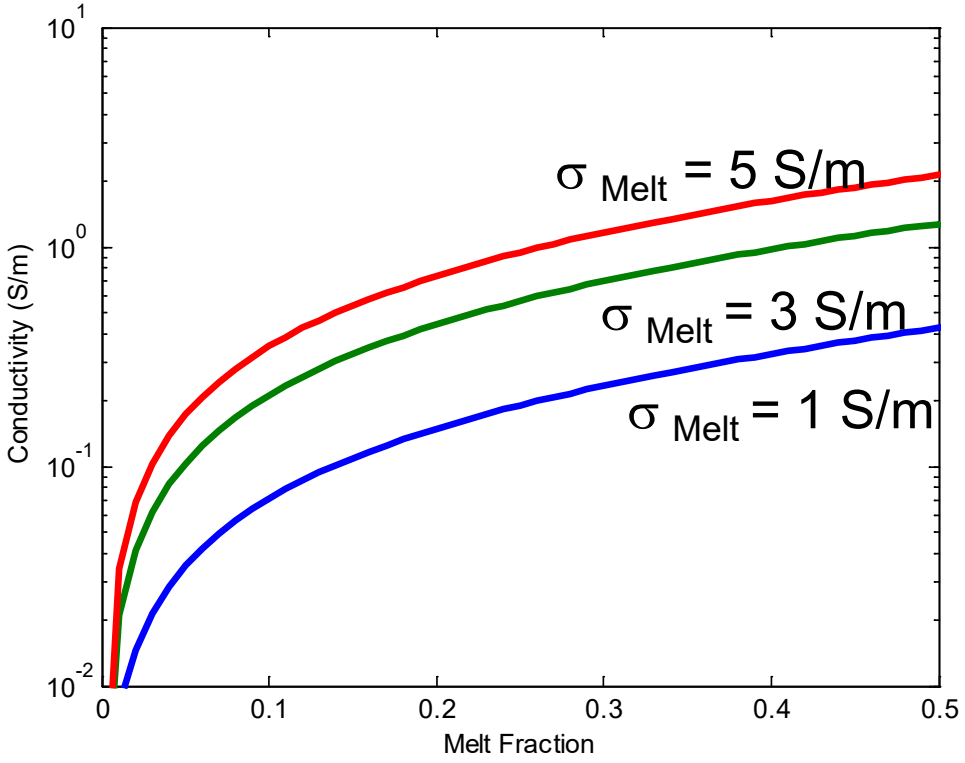

Using the formalism of Schilling et al. 1997, Physics of Earth and Planet. Interiors

$$\sigma = \frac{\sigma_l\left(\sigma_l\left(f^{2/3}-1\right)-\sigma_s f^{2/3}\right)}{\sigma_s\left(f-f^{2/3}\right)+\sigma_l\left(f^{2/3}-f-1\right)}$$

Where x is volume melt fraction, f = 1-x, σ_1 is conductivity of the melt and σ_s is the conductivity of the solid rock

I24 Data, MHD, solid mantle, Magma ocean

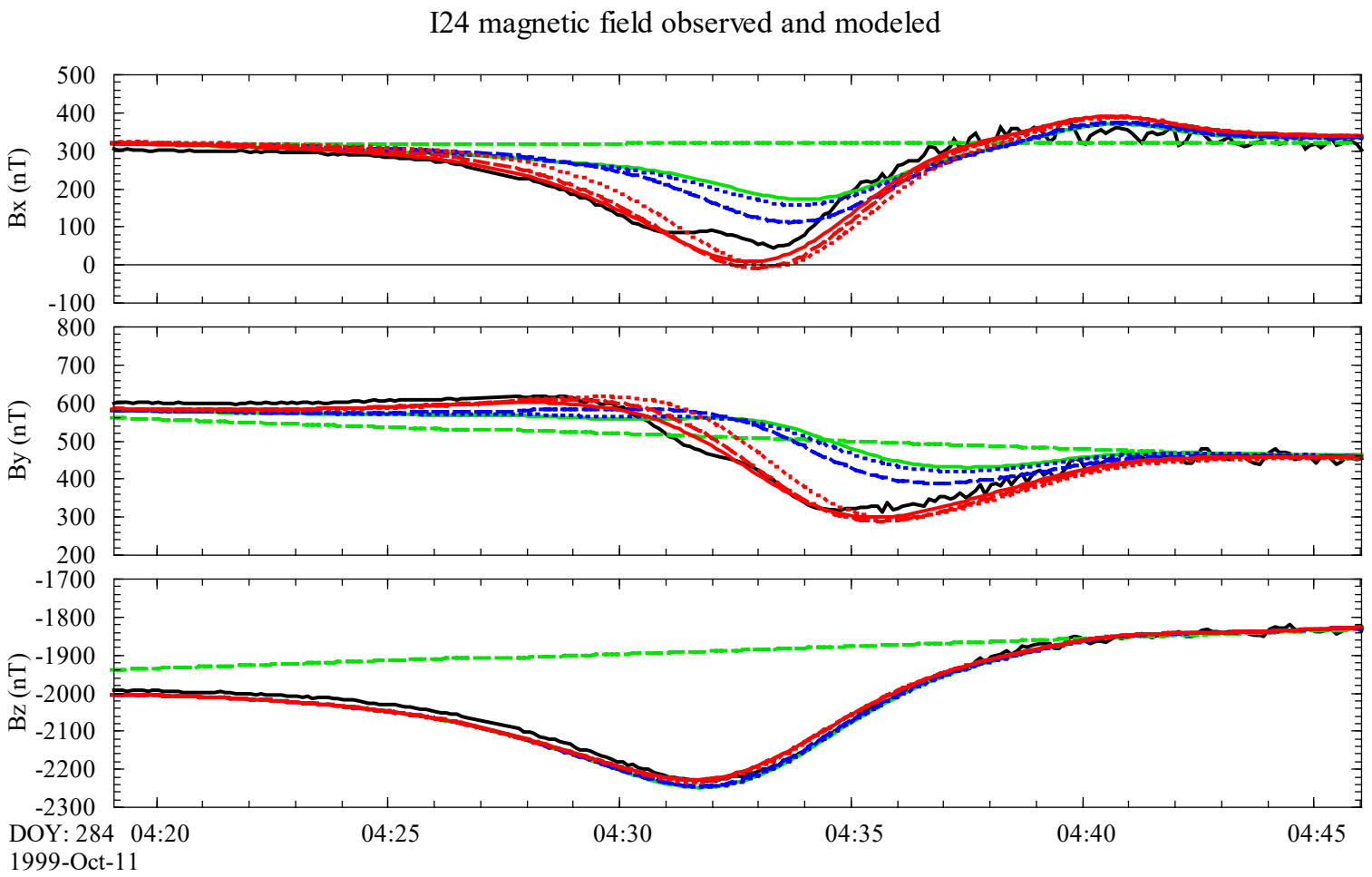

Khurana et al. 2011, Science

Melt fraction for three magma ocean models is 5%, 20% and 100%
Thickness = 50 km.

Model predicted dipole moment vs. observed for all four flybys

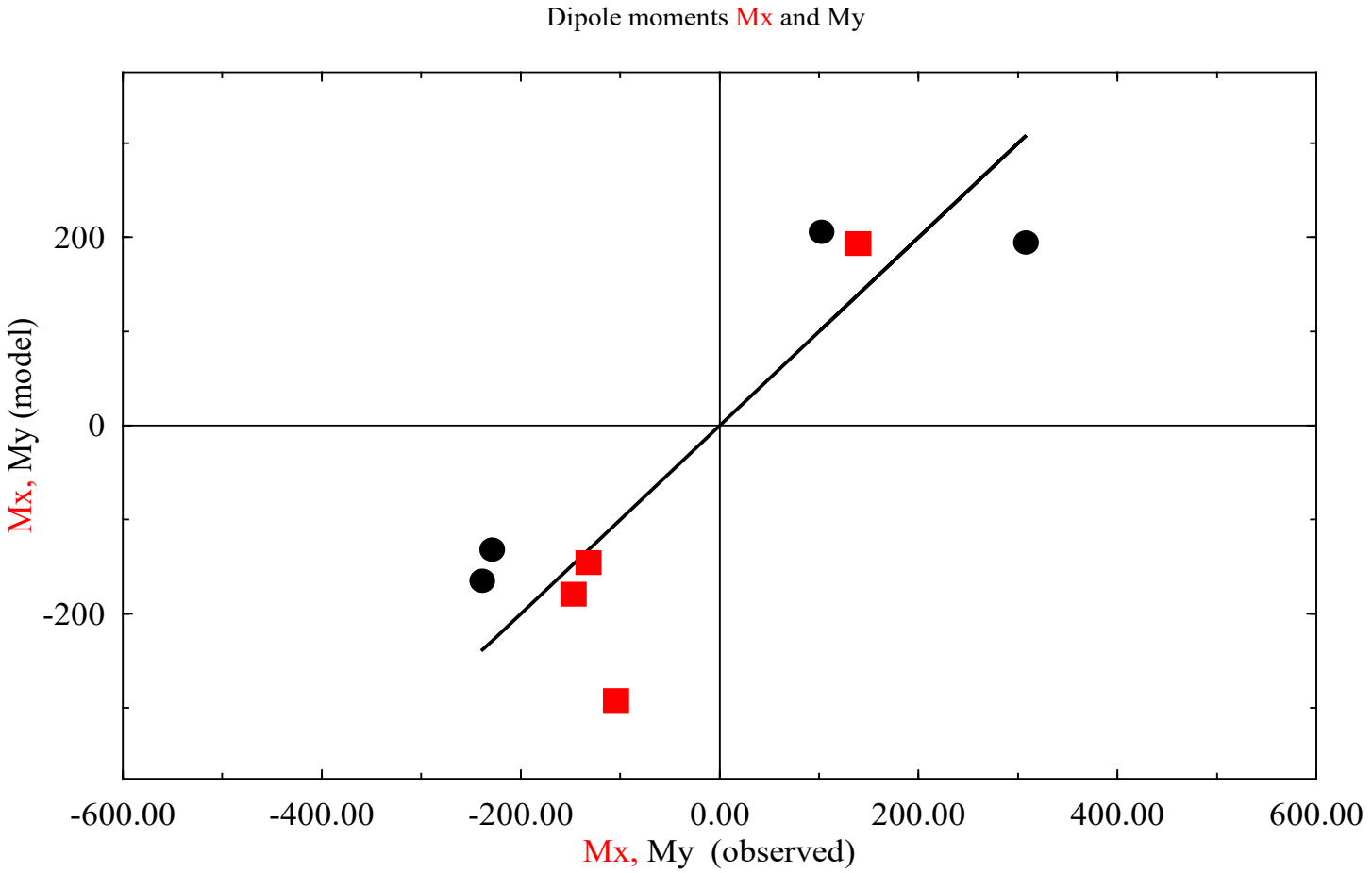

Khurana et al. 2011, Science

Io Volcano Observer

Alfred McEwen
University of Arizona,
partnered with APL

Lunar and Planetary Laboratory, University of Arizona
The Johns Hopkins University Applied Physics Laboratory
University of Bern
Swedish Institute of Space Physics
Jet Propulsion Laboratory
University of California at Los Angeles
German Aerospace Center

Expected and recovered internal and external harmonics

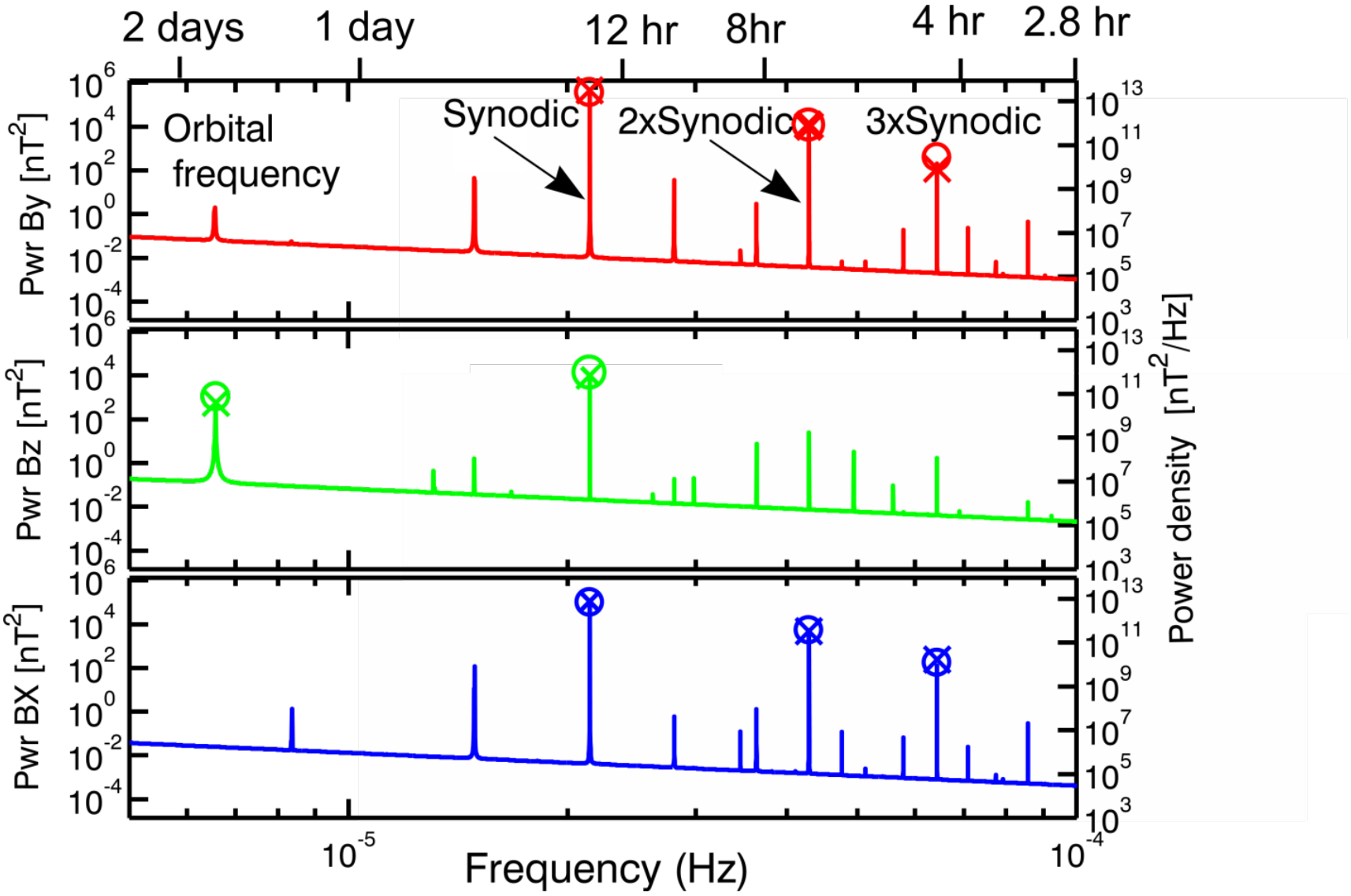

Io Conclusions

- The Galileo magnetic field data from I24, I27, I31 and I32 passes are consistent with models that require large melt fractions (~ 20%) of rocks in the asthenosphere of Io suggesting that a contemporaneous global magma ocean exists in Io. The thickness of the melt layer is at least 50 km.

- The permanent dipole and quadrupole terms from the internal dynamo field are small (< 110 nT, polar surface field).

Reserve Slides Follow

Future work (Multi-frequency induction)

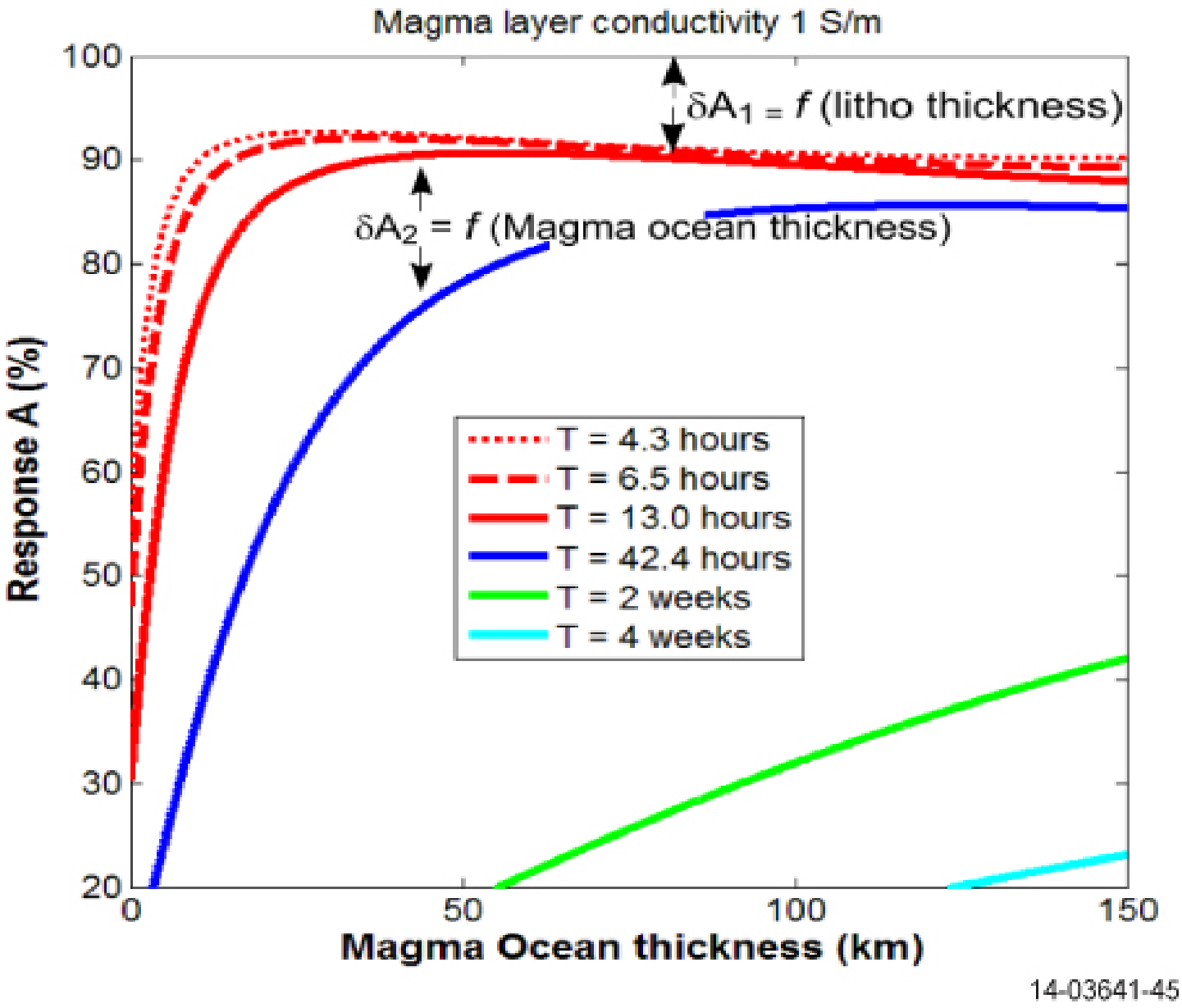

Future work: Determining magma ocean thickness

RED Io's response (polar, nT) at synodic rotation period

Blue: Io's response at orbital period of Io

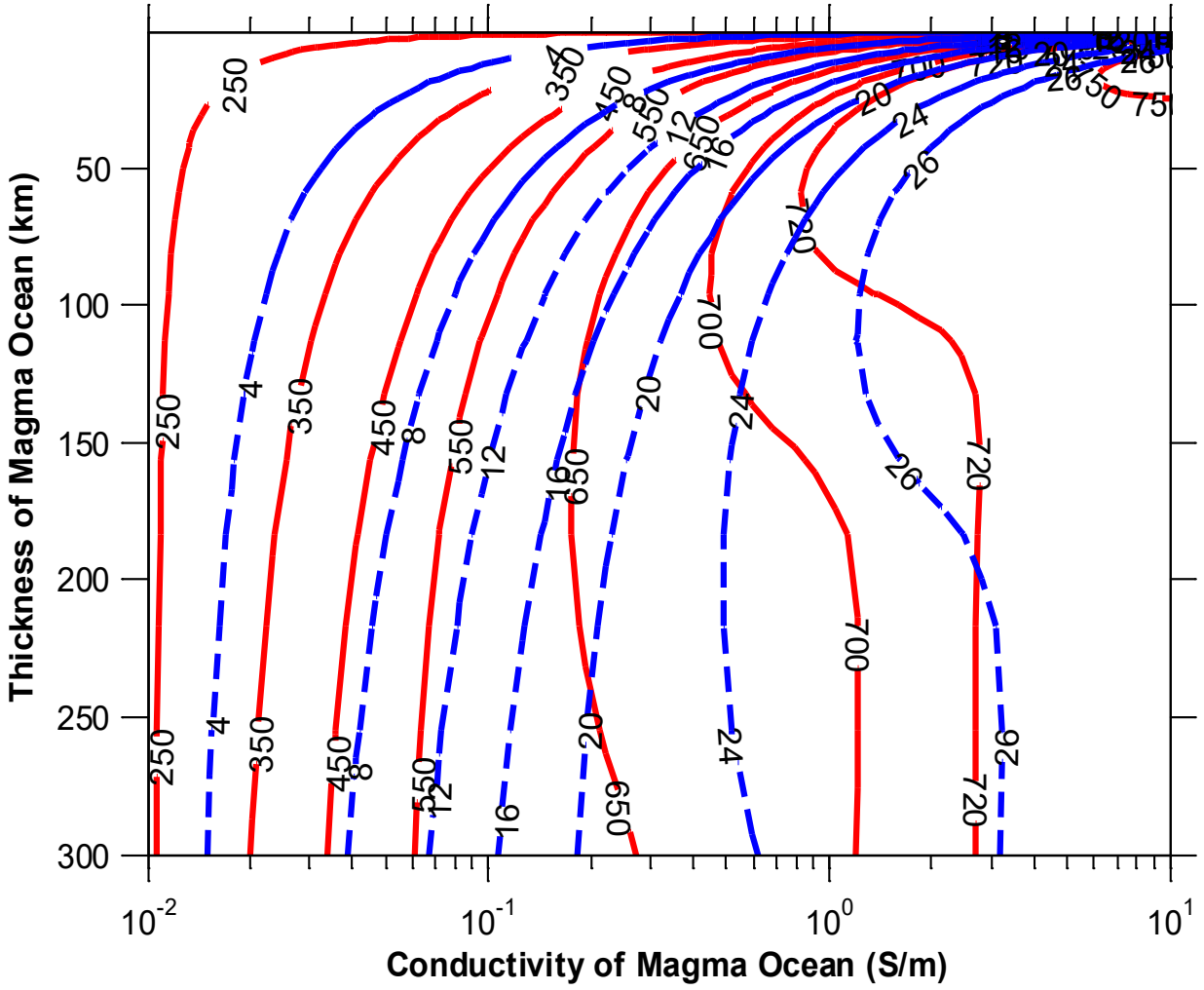

Induction from core + mantle

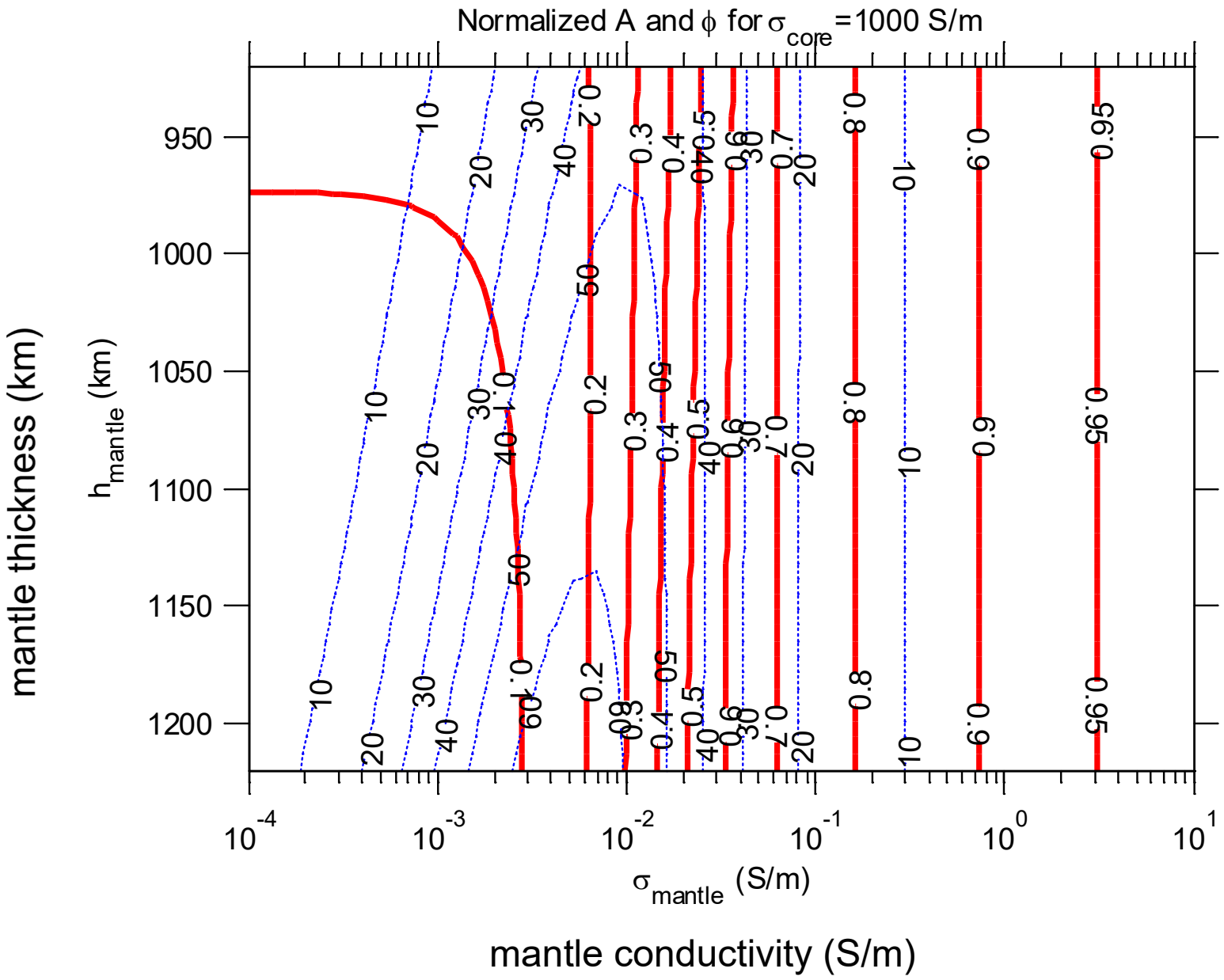

Induction from core + mantle
Extended range plot

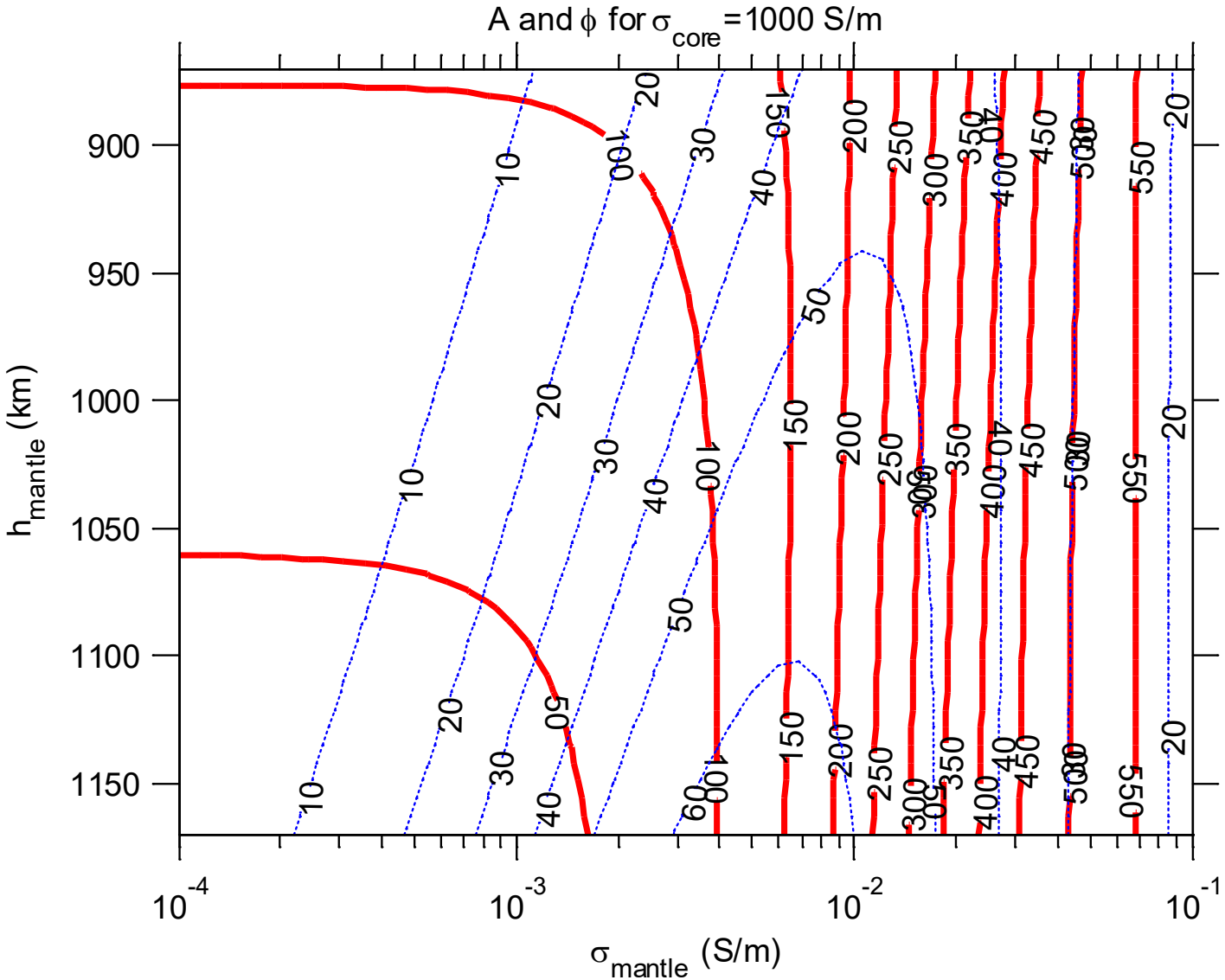

Expectations for induction field from Io: Lava conductivities

Table 9. Melt conductivity needed to model the measured molten rock conductivity with Hashin-Strikman upper bound (Eqn. 8).

Sample	$T_{quenching}$ (°C)	log (σ_{solid}) (S/m)	σ_{melt} (S/m)	X_{melt} (vol.%)	log (σ_{HS^+}) (S/m)	log (σ_{mes}) (S/m)
Oman gabbro						
1 GPa	1240	–2.08	1.5	34	–0.41	–0.4
0.5 GPa	1188	–2.24	0.29	15	–1.44	–1.45
0.5 GPa	1187	–2.25	0.31	12	–1.51	–1.5
0.3 GPa	1196	–2.22	0.48	17	–1.20	–1.2
Karelia olivinite, 1 GPa	1315	–1.92	28.8	10	0.30	0.3
Spitzbergen lherzolite						
2 GPa	1465	–1.86	4.9	22	–0.10	–0.1
1 GPa	1360	–2.25	2.5	14	–0.60	–0.6
Ronda lherzolite, 1 GPa	1377	–2.25	2.0	11	–0.80	–0.8
Ol + basalt sample, 1 GPa	1183	–3.06	2.9	4.5	–1.05	–1.05

Induction from core + mantle

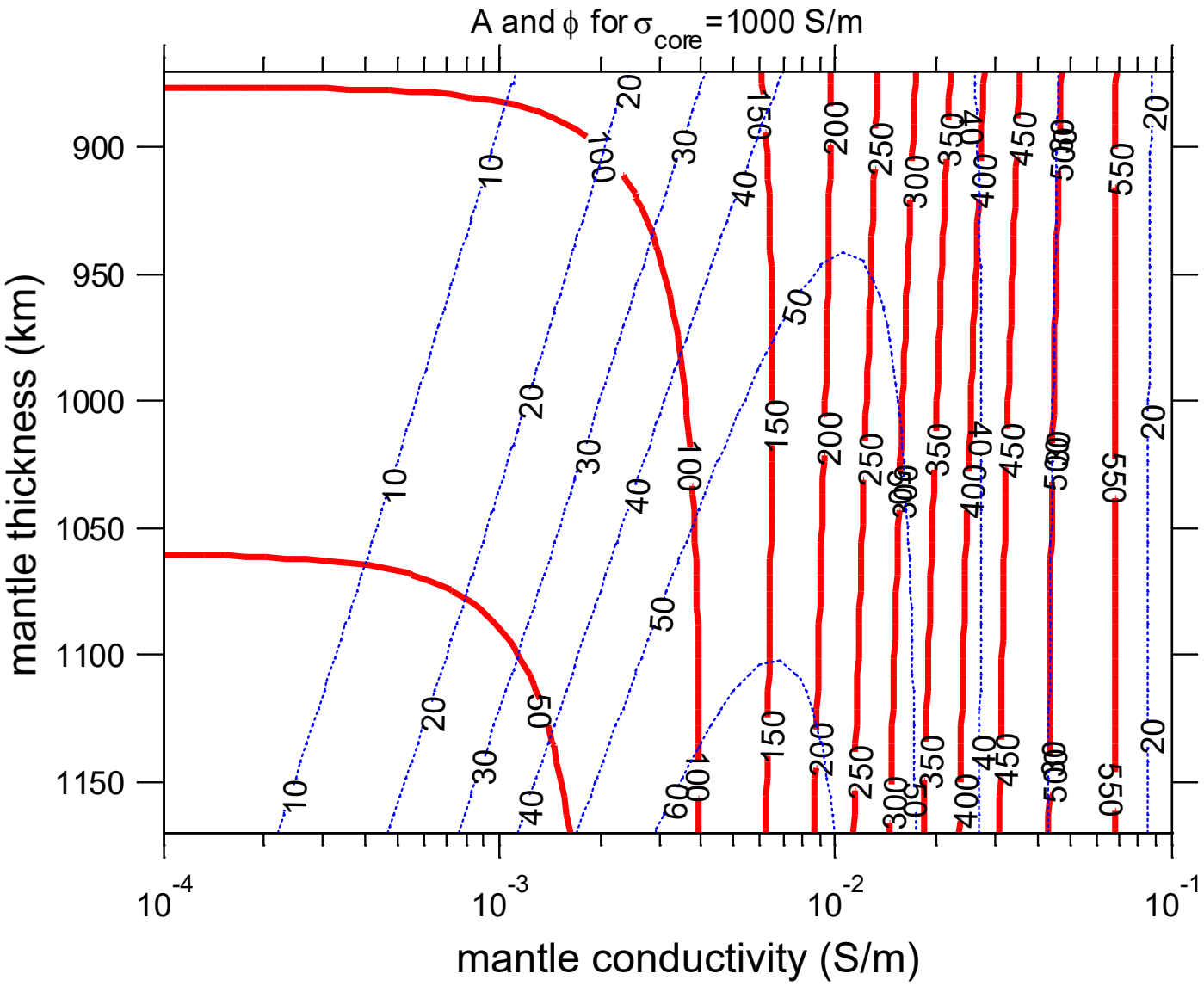

Three layer model

- Assume crust thickness d = 50 km electrically insulating
- r_m = 1820 km
- r_0 = 1770 km.
- Core radius r_1 = 600 – 900 with ∞ conductivity.
- Mantle thickness h = r_0 - r_1 = 870 – 1170 km with a range of conductivities.

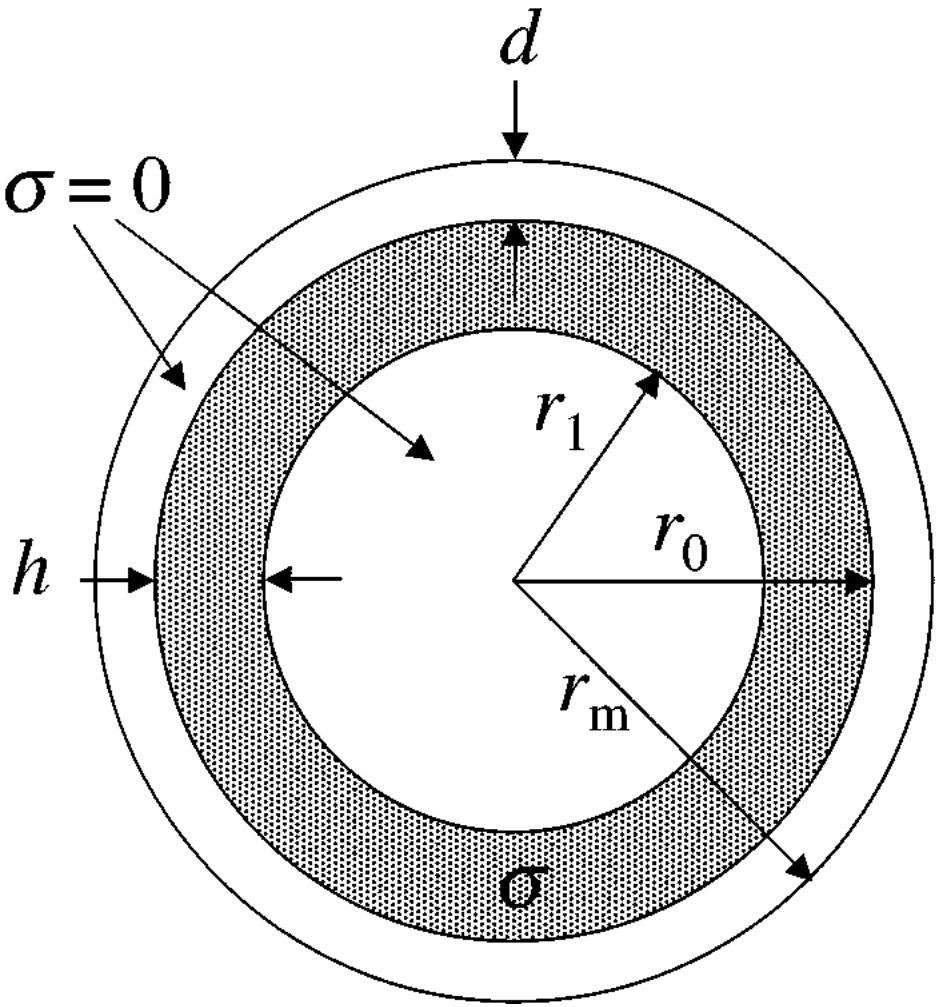

Expectations for induction field from Io: Conductivities of rocks with melt fractions

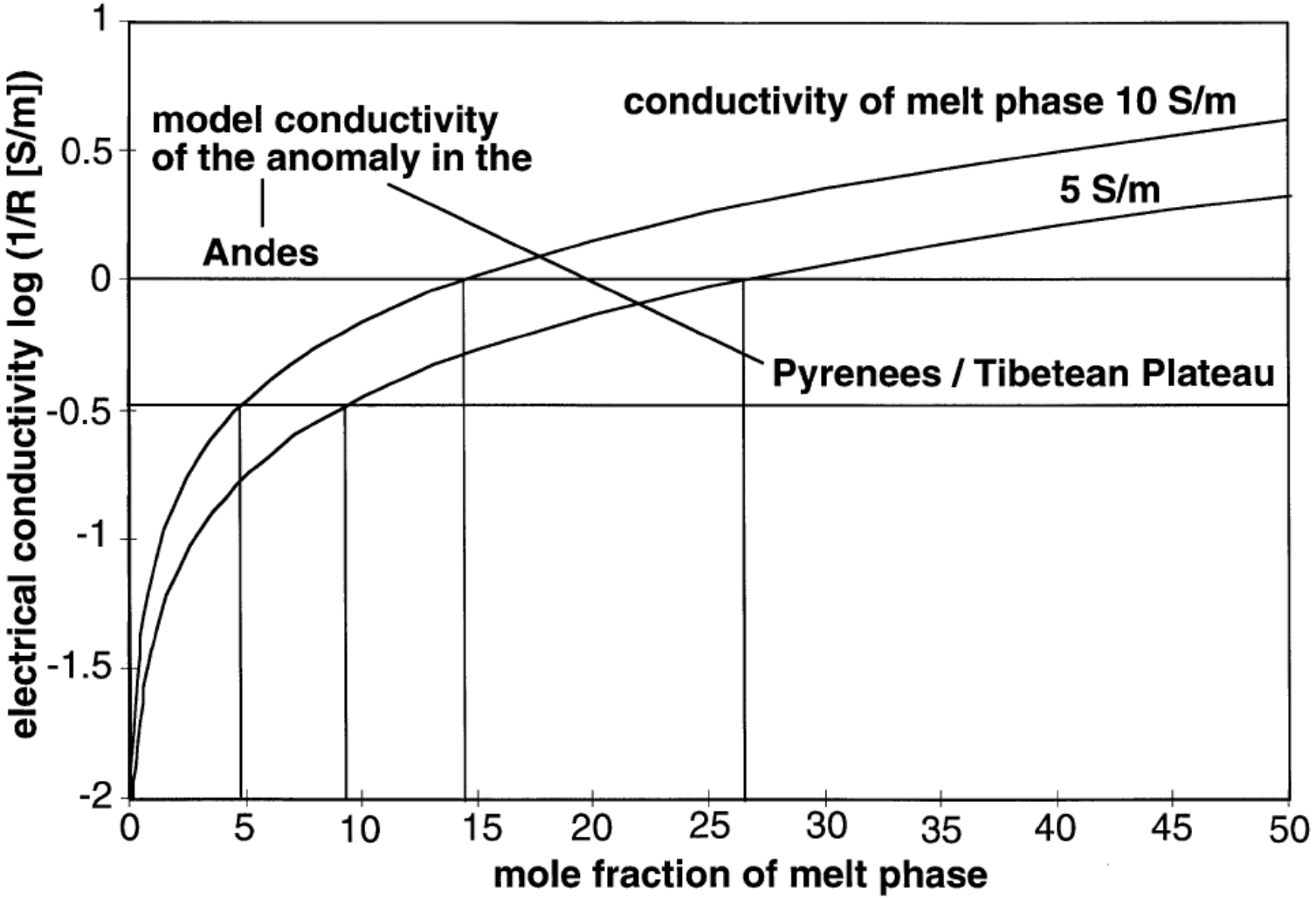

Molten rocks have very “high” conductivity

Table 9. Melt conductivity needed to model the measured molten rock conductivity with Hashin-Strikman upper bound (Eqn. 8).

Sample	$T_{quenching}$ (°C)	log (σ_{solid}) (S/m)	σ_{melt} (S/m)	X_{melt} (vol.%)	log (σ_{HS^+}) (S/m)	log (σ_{mes}) (S/m)
Oman gabbro						
1 GPa	1240	–2.08	1.5	34	–0.41	–0.4
0.5 GPa	1188	–2.24	0.29	15	–1.44	–1.45
0.5 GPa	1187	–2.25	0.31	12	–1.51	–1.5
0.3 GPa	1196	–2.22	0.48	17	–1.20	–1.2
Karelia olivinite, 1 GPa	1315	–1.92	28.8	10	0.30	0.3
Spitzbergen lherzolite						
2 GPa	1465	–1.86	4.9	22	–0.10	–0.1
1 GPa	1360	–2.25	2.5	14	–0.60	–0.6
Ronda lherzolite, 1 GPa	1377	–2.25	2.0	11	–0.80	–0.8
Ol + basalt sample, 1 GPa	1183	–3.06	2.9	4.5	–1.05	–1.05

I27 Data, MHD

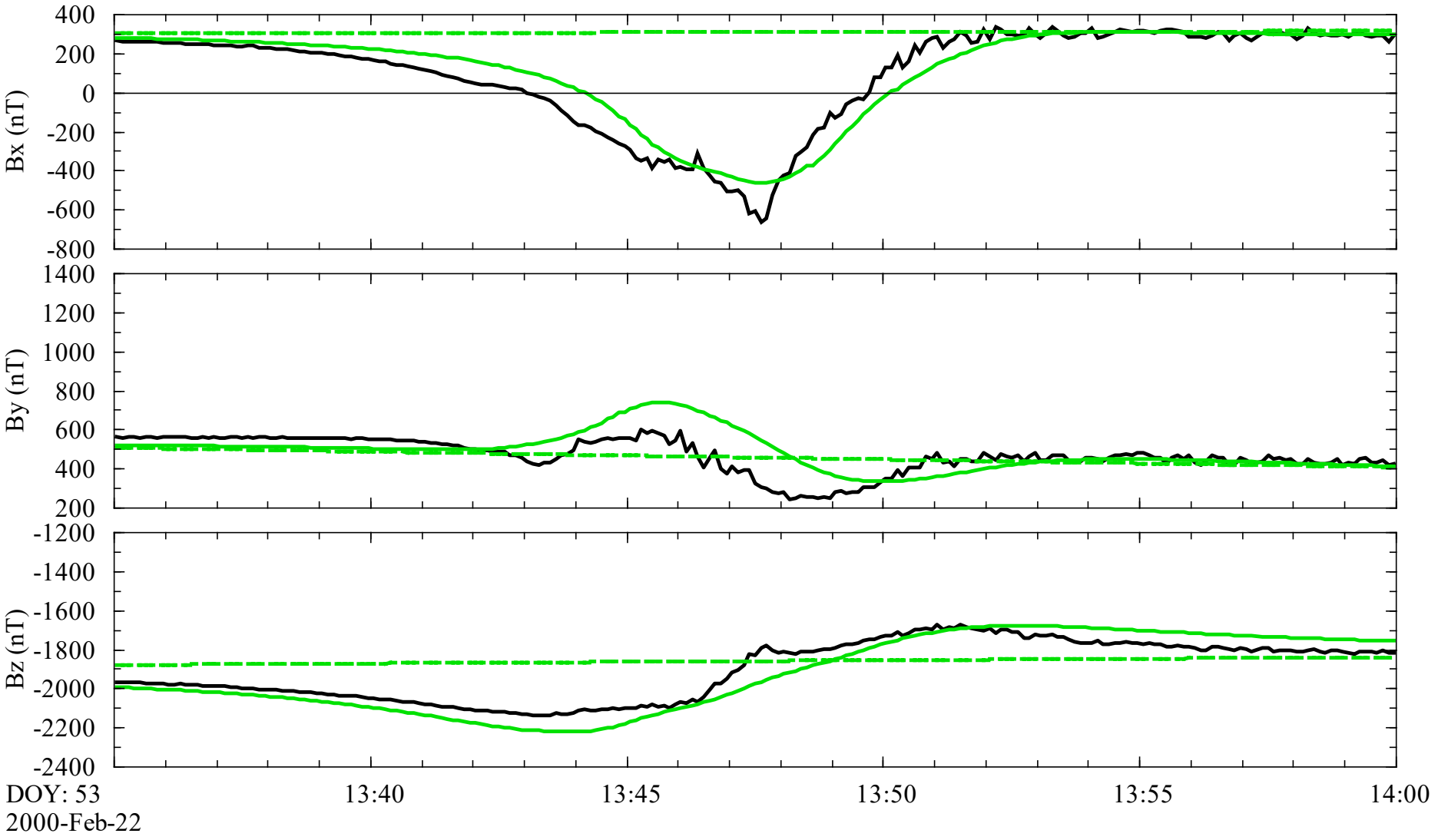
Bx (nT)
400
200
0
-200
-400
-600
-800
By (nT)
1400
1200
1000
800
600
400
200
Bz (nT)
-1200
-1400
-1600
-1800
-2000
-2200
-2400
DOY: 53
2000-Feb-22
13:40
13:45
13:50
13:55
14:00

I27 Data, MHD, solid mantle

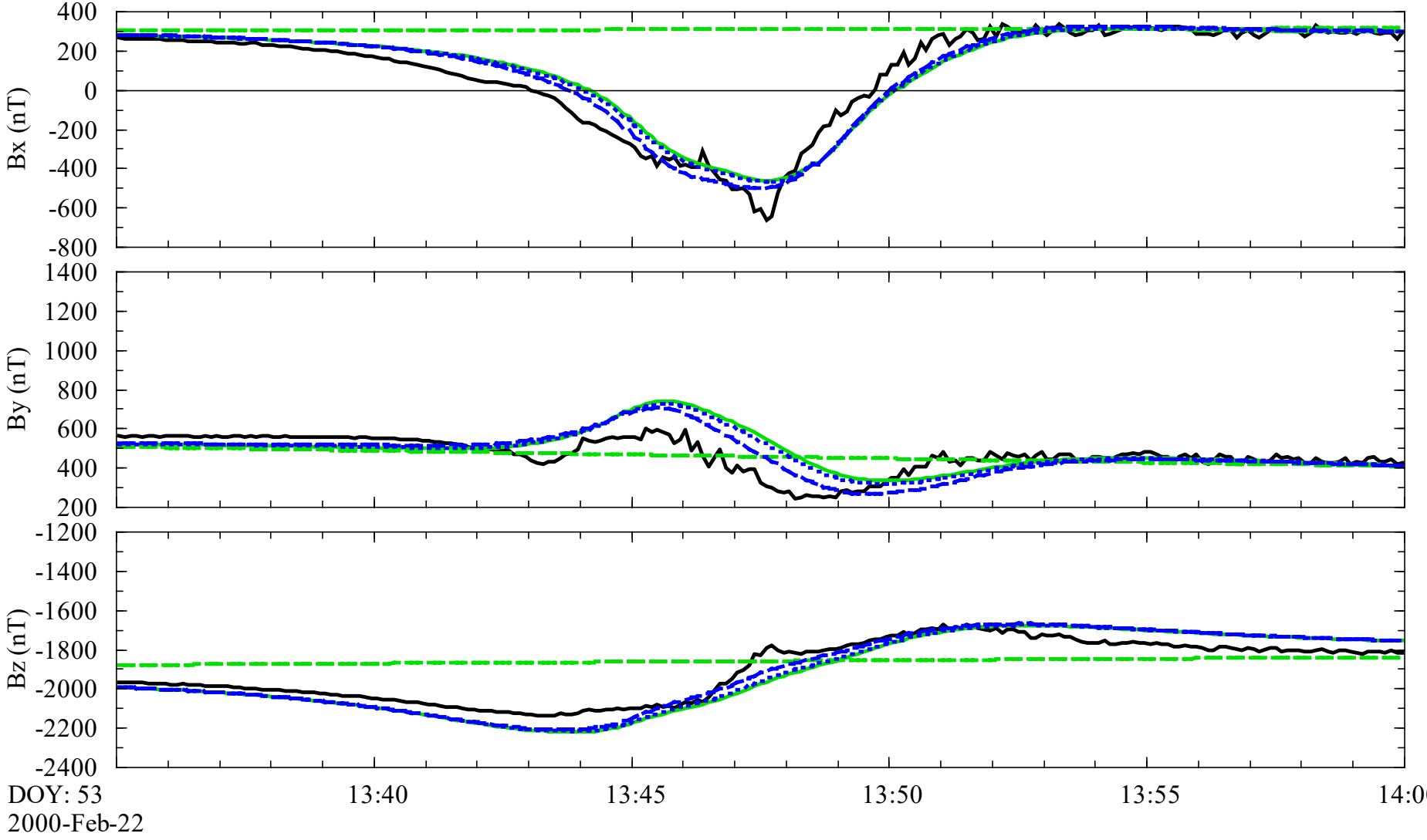

Induction from a magma ocean overlying solid mantle

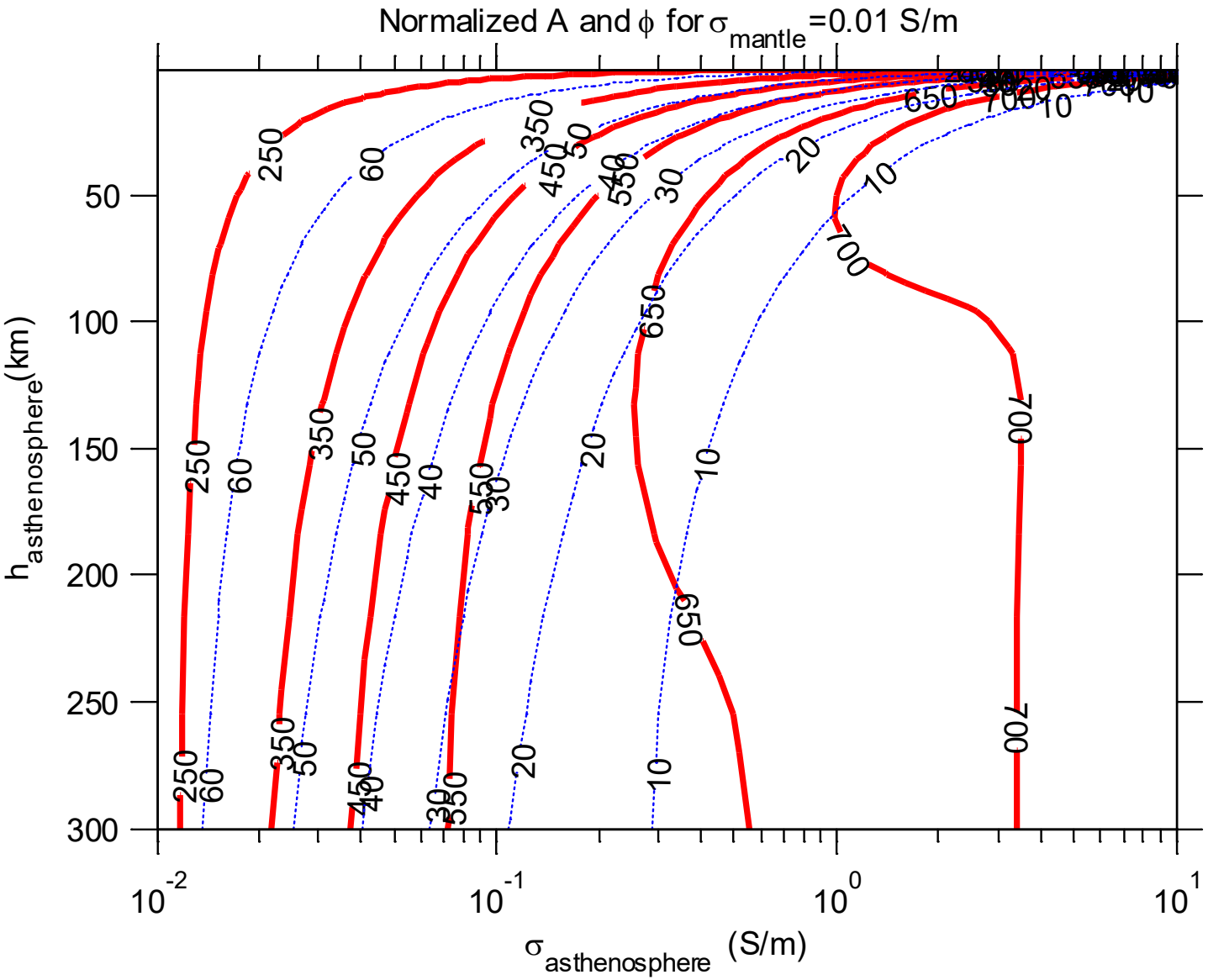

3D MHD Simulation Model

We use a modified version of Linker's Io code with improved boundary conditions.

The code includes charge exchange, electron impact ionization and Pedersen conductivity profiles defined by scale height of neutrals (assumed spherically symmetric) and density of charged species (obtained self consistently from simulations).

The total ionization rate is about 4.4*10e27 ions/s and total charge exchange is about 1.5*10E28 for I24.

- A $131\times132\times128\,(r,\theta,\varphi)$ non-uniform spherical mesh covering a calculation domain $0.5R_{Io} < r < 25R_{Io}$ with fine grids (~ $0.02R_{Io}$ or 40 km) near Io.

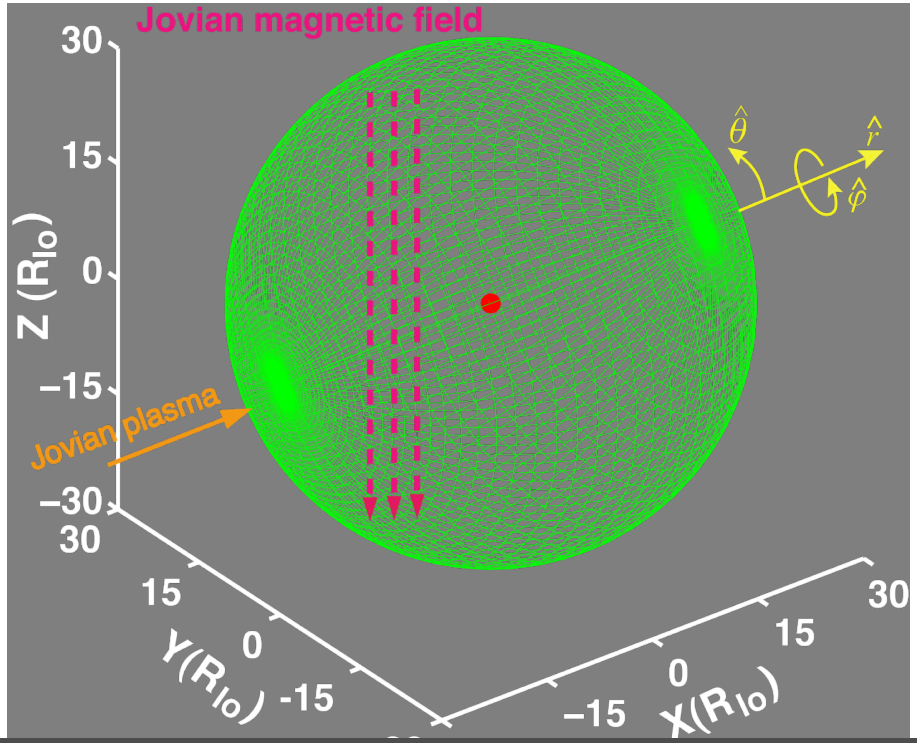

$$\frac{\partial \rho}{\partial t} + \nabla \cdot (\rho \mathbf{v}) = \dot{\rho}_s$$

$$\rho\left(\frac{\partial \mathbf{v}}{\partial t} + \mathbf{v}\cdot\nabla\mathbf{v}\right) = -\nabla P + \mathbf{J}\times\mathbf{B} - \dot{\rho}_s\mathbf{v} - \dot{Q}_s\mathbf{v}$$

$$\frac{\partial P}{\partial t} + \nabla\cdot(P\mathbf{v}) = (\gamma-1)\left(-P(\nabla\cdot\mathbf{v}) + \eta J^2 + \frac{\dot{\rho}_s v^2 + \dot{Q}_s v^2}{2}\right) - \frac{\dot{Q}_s P}{\rho}$$

$$\frac{\partial \mathbf{A}}{\partial t} - \mathbf{v}\times(\nabla\times\mathbf{A}) = -\eta\nabla\times(\nabla\times\mathbf{A})$$

$$\mathbf{B} = \nabla\times\mathbf{A}\ ,\ \mathbf{J} = \nabla\times\mathbf{B}$$

where $\dot{\rho}_s = MN_n/\tau$, $\dot{Q}_s = \sigma\rho N_n|\mathbf{v}|$, $N_n = N_0\exp(-\frac{r-r_0}{h_s})$

Background field and plasma conditions used in the MHD simulations were obtained from observations.

	I0	I24	I27	I31	I32
Bx (nT)	0	0	0	0	0
By (nT)	-96	518	497	-670	-240
Bz (nT)	-1804	-1906	-1878	-1967	-1813
Ne (/cc)	3850	500	700	1200	3170
V (km/s)	57	57	57	57	57
T (eV)	100	30	100	100	100

I27 Data, MHD, solid mantle, Magma ocean

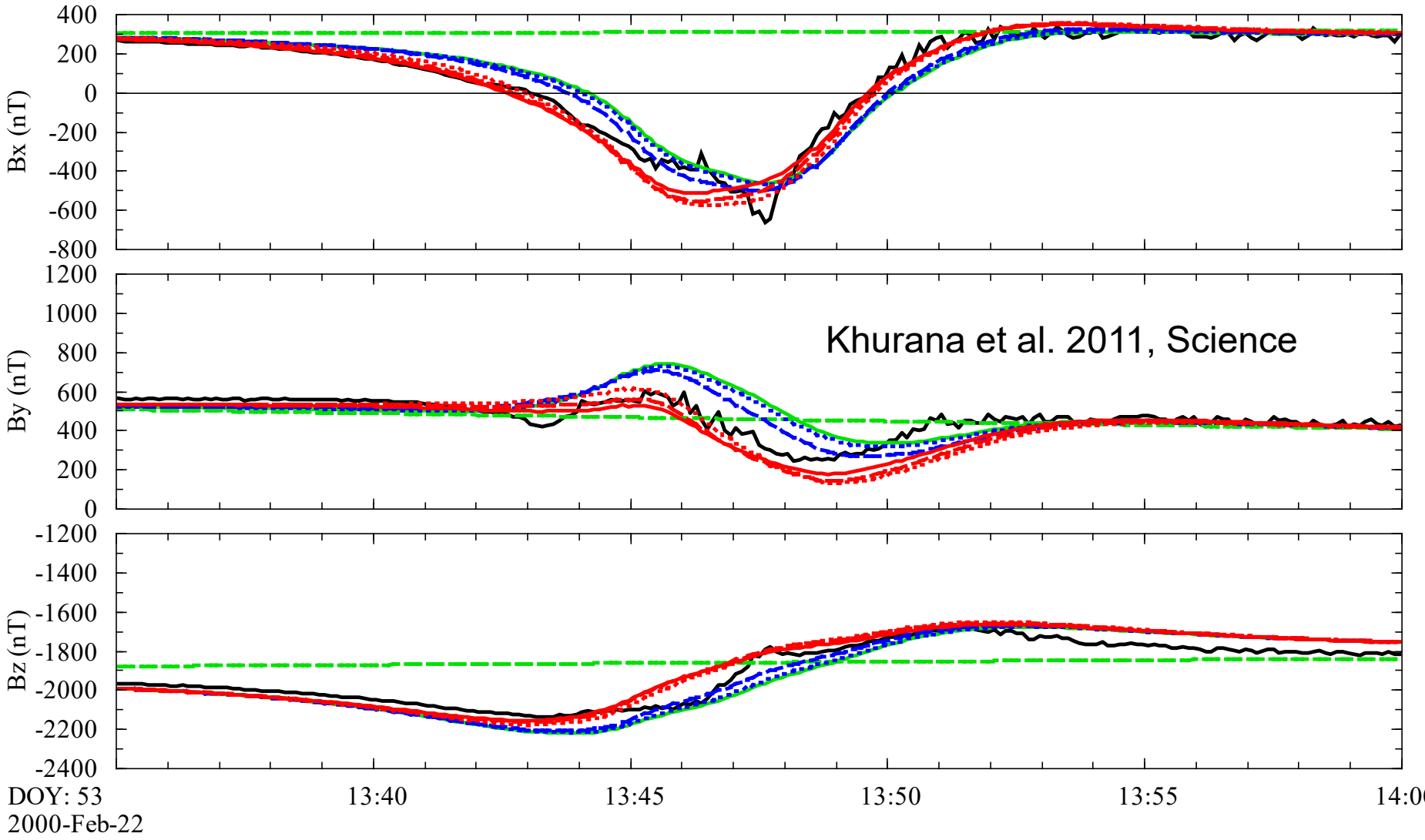

Melt fraction for three magma ocean models is 5%, 20% and 100%

The principle behind electromagnetic induction
Moon's with internal conductivity (liquid oceans, magma oceans)

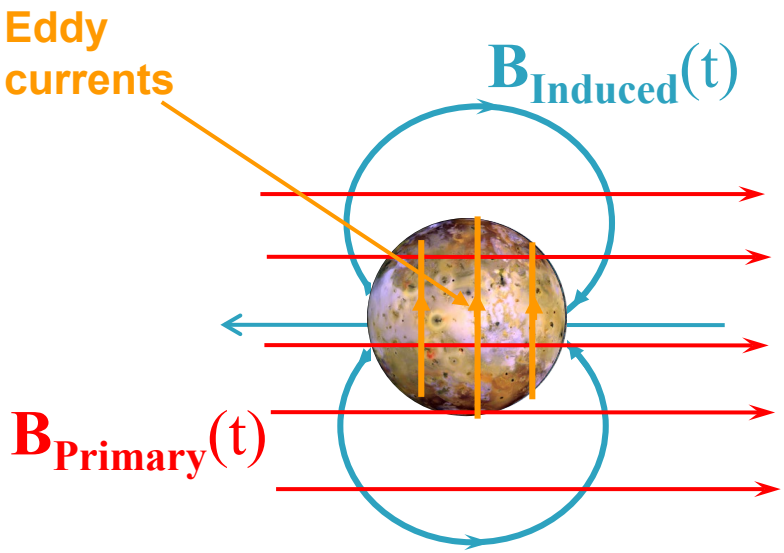

The primary and secondary fields shown separately

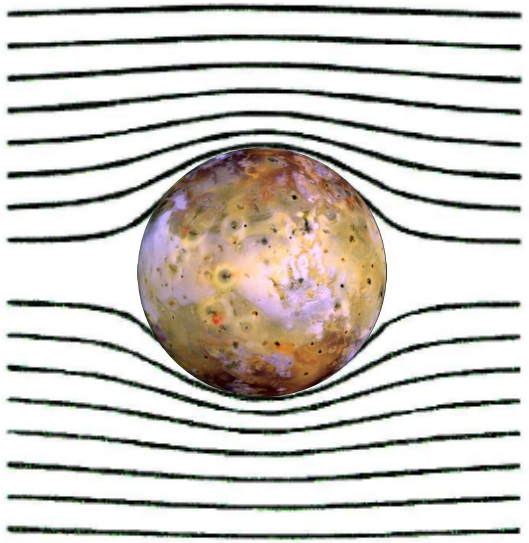

The primary and secondary fields summed together

–Eddy currents generate a secondary or induced field which reduces the primary field inside the conducting magma ocean.

–The induced field can be detected with a sensor.

Callisto ocean

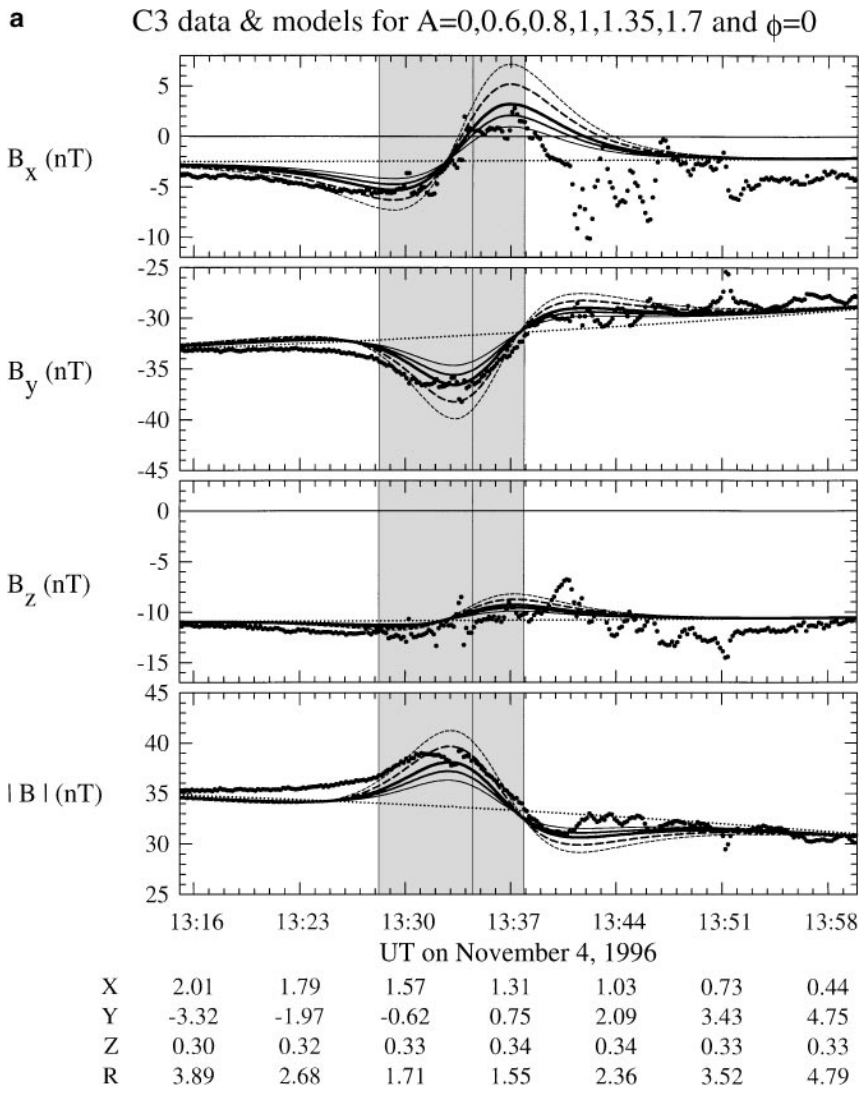

X	2.01	1.79	1.57	1.31	1.03	0.73	0.44
Y	-3.32	-1.97	-0.62	0.75	2.09	3.43	4.75
Z	0.30	0.32	0.33	0.34	0.34	0.33	0.33
R	3.89	2.68	1.71	1.55	2.36	3.52	4.79

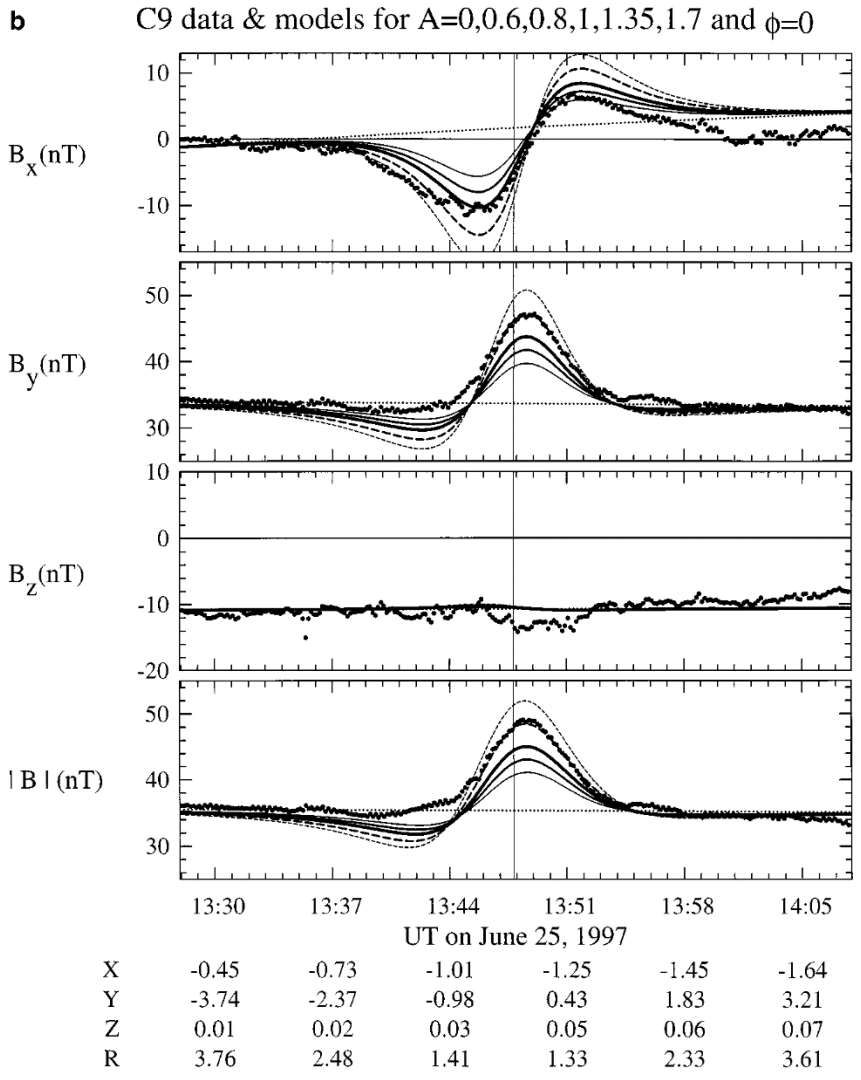

X	-0.45	-0.73	-1.01	-1.25	-1.45	-1.64
Y	-3.74	-2.37	-0.98	0.43	1.83	3.21
Z	0.01	0.02	0.03	0.05	0.06	0.07
R	3.76	2.48	1.41	1.33	2.33	3.61